SEPARATION OF CO_2 AND H_2 MIXTURES USING REACTIVE ION EXCHANGE MEMBRANES

by

J. Douglas Way and R. Lane Hapke
SRI International
Chemical Engineering Laboratory
Menlo Park, CA 94025.

Introduction

Currently, the most widely used method for producing hydrogen is steam reforming of methane. The volatility in the price of natural gas has created increased interest in finding alternative feedstocks for the manufacture of hydrogen. Thus, it is appropriate at this time to conduct research which has the best opportunities for reducing H_2 production costs from coal gasification.

Bartis and Marks (1984) have identified low energy separation processes such as membranes as a key research opportunity in reducing capital and operating costs and hence the H_2 production costs. They state that technical improvements in gas separation could lead to production cost reductions of 15 to 20 percent. Figure 1 is a block flowsheet of a process to produce hydrogen from synthesis gas. There are two points in the process where gas separation processes take place. Acid gases must be removed from the gas stream after gasification and prior to the shift reaction. This separation step prevents sulfur poisoning of the shift catalysts and maximizes hydrogen production from the shift reaction. The second gas separation occurs after the shift reaction. CO_2 must be removed from the product stream to produce high purity H_2.

Membrane Separations

The use of membrane separations for the gas separation processes described above is an area deserving special attention because of its great potential for low capital cost and energy efficiency (Matson et al., 1983). A membrane process could theoretically separate a binary mixture reversibly, and therefore consume only the minimum work to accomplish the separation. The implicit simplicity and energy

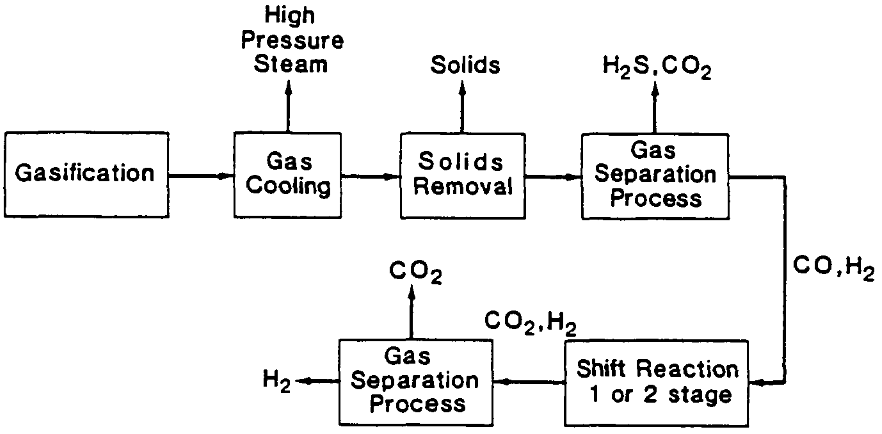
High Pressure Steam
Solids
H_2S, CO_2
Gasification
Gas Cooling
Solids Removal
Gas Separation Process
CO, H_2
CO_2
CO_2, H_2
H_2
Gas Separation Process
Shift Reaction 1 or 2 stage

RA-m-360583-34

FIGURE 1 BLOCK FLOW DIAGRAM OF HYDROGEN PRODUCTION FROM SYNTHESIS GAS

efficiency of membrane processes have stimulated basic and applied research for many years.

The selective removal of CO_2 from mixtures of H_2, CO, and other gasification products using membranes depends on the appropriate choice of the membrane material. Many glassy polymers commonly used in commercial gas separation membranes are more permeable to H_2 than CO_2. The ideal separation factor, $\alpha(H_2/CO_2)$ for commercial asymmetric cellulose ester membranes is 2.2 (W. R. Grace, 1986) while the value for the polydimethylsiloxane/polysulfone composite membranes is 2.3 (Henis and Tripodi,1980). Due to the large diffusivity of H_2 in typical glassy polymer materials the permeability coefficient (product of the diffusivity and solubility) of H_2 is greater than that of CO_2. While diffusivity controls the selectivity in glassy polymers, in rubbery polymers such as polydimethylsiloxanes (PDMS) or PDMS copolymers the solubility of penetrant gases controls the selectivity. In this case, the selectivity of the rubbery polymer membranes is reversed, and the membranes are more permeable to CO_2 than to H_2. The ideal separation factors (CO_2/H_2) are 4.9 and 4.6 for PDMS and PDMS/polycarbonate copolymers, respectively (Robb, 1968; General Electric, 1982). A separation factor of 6.4 was measured using a commercial GE PDMS membrane with a 50/50 mole % CO_2/H_2 feed gas mixture at ambient conditions. The measured CO_2 permeability was 2310 Barrer (1 Barrer=10^{-10} $cm^3(STP)cm/cm^2 \cdot s \cdot cm$ Hg) which is within 7% of the pure component value (General Electric, 1982). However, the H_2 permeability was 359 Barrer, only 70% of the pure component value. This observation could be explained if the H_2 solubility, and therefore the permeability, during the mixture experiment is lower than the pure component value due to the presence of CO_2 in the membrane.

Facilitated Transport Membranes

Liquids and solvent swollen ionomer membranes can also be used as membrane materials (Ward and Robb, 1968; LeBlanc et al., 1980; Way et al., 1987).

Incorporation of a complexation agent in these membranes can enhance the flux of a reactive species through a process known as facilitated transport. Way et al. (1987) have demonstrated facilitated transport of CO_2 through water-saturated perfluorosulfonic acid ion exchange membranes (IEMs) containing monopositive ethylene diamine as a counterion.

Ion exchange membranes containing EDA were prepared using the method of Way et al. (1987) using nominal 30 µm NE-111 perfluorosulfonic acid membranes. The experimental NE-111 membranes have an equivalent molecular weight of 1100 g/eq and are not available commercially. Preliminary transport measurements were performed at 25 °C and 1 atm to determine the CO_2 and H_2 permeabilities of the NE-111 IEMs. The pure component CO_2 permeability was 145 Barrer, in good agreement with the value of 146 Barrer previously reported by Noble et al. (1988). The H_2 permeability was 21.2 Barrer, corresponding to an ideal separation factor of 6.84 for the NE-111 IEM. The ideal separation factor for water, calculated by determining the ratio of permeability coefficients, is 17.2 at 25 °C and 1 atm (Kohl and Riesenfeld, 1985; Cussler, 1984). A possible explanation of the lower separation factor for the water-swollen IEM is that H_2 may diffuse through both the water containing cluster-channel network phase of the IEM (Gierke, 1977) and the fluorocarbon polymer phase. Further experiments will be performed to determine the permeability and separation factor for mixtures of CO_2 and H_2 using water as a solvent.

Selectivity improvements may be obtained by preparing facilitated transport IEMs using polar organic solvents such as propylene carbonate which are used commercially in physical absorption processes for removing CO_2 from gas mixtures. Propylene carbonate has the property that CO_2 is 121 times more soluble than H_2 at ambient conditions (Kohl and Riesenfeld, 1985). Assuming that the ratio of the diffusion coefficients (CO_2/H_2) in propylene carbonate is the same as water, an ideal separation factor (CO_2/H_2) of approximately 50 can be calculated.

Summary

Liquids and rubbery polymers are good candidate membrane materials for the separation of CO_2 from mixtures with H_2 because the solubility selectivity controls the separation that can be obtained. Facilitated transport IEMs containing monopositive ethylene diamine counterions have been shown to be selectively permeable to CO_2 over H_2. Transport measurements will be conducted to determine the influence of feed gas mixture composition, pressure, temperature, and solvent on the CO_2 and H_2 permeabilities and separation factor.

Acknowledgement

The authors would like to ackowledge the support of the Dept. of Energy Morgantown Energy Technology Center for this work under subcontract NB773000707471 to DOE Contract No. DE-AI21-86MC23120, with special thanks to Ms. Lisa A. Jarr. We would also like to acknowledge Dr. Louis L. Burton of E. I. duPont de Nemours & Co., Inc., for supplying developmental forms of perfluorinated ion exchange membranes.

References

Bartis , J. T., and L. S. Marks, "Technical Evaluation and Systems Analysis of Hydrogen Production from Coal," Final Report for DOE Contract No. DE-AP21-84MC02159 (August, 1984).

Cussler, E. L., *Diffusion: Mass Transfer in Fluid Systems*, Cambridge University Press, Cambridge (1984).

General Electric Membrane Products Operation, General Electric Permselective Membranes Product Literature, 1982.

Gierke, T. D., "Ionic Clustering in Nafion Perfluorosulfonic Acid Membranes and Its Relationship to Hydroxyl Rejection and Chlor-Alkali Current Efficiency," Proc. Electrochemical Society Meeting, Atlanta, GA,1977.

Grace Membrane Systems, Performance Specifications, 1986.

Henis, J. M. S., and M. K. Tripodi, U. S. Patent 4,230,463 (1980).

Kohl, A. L., and F. C. Riesenfeld, *Gas Purification*, 4th Edition, Gulf Publishing Co., Houston (1985).

LeBlanc, O. H., Ward, W. J., Matson, S. L., and S. G. Kimura, "Facilitated Transport in Ion Exchange Membranes," *J. Mem. Sci.*, **6**, 339-343(1980).

Matson, S. L., Lopez, J. and J. A. Quinn, "Separation of Gases With Synthetic Membranes," *Chem. Eng. Sci.*, **38**, 503-524(1983).

Noble, R. D., Pellegrino, J. J., Grosgogeat, E., Sperry, D., and J. D. Way, "CO_2 Separation Using Facilitated Transport Ion Exchange Membranes," *Sep. Sci. Tech.*, accepted for publication, 1988.

Robb, W. L., "Thin Silicone Membranes-Their Permeation Properties and Some Applications," *Ann. N. Y. Acad. Sci.* **146**, 119-137(1968).

Ward, W. J., W. L. Robb, "Carbon Dioxide-Oxygen Separation: Facilitated Transport of Carbon Dioxide Across a Liquid Film," *Science*, **156**, 1481(1967).

Way, J. D., Noble, R. D., Flynn, T. M., and E. D. Sloan, "Liquid Membrane Transport: A Survey," *J. Mem. Sci.*, **12**, 239-259(1982).

SEPARATIONS OF OLEFINS AND HETEROCYCLIC ORGANIC COMPOUNDS BASED ON REVERSIBLE COMPLEXATION REACTIONS.

Carl A. Koval[1], Steven Drew[1], Terry Spontarelli[1], Richard D. Noble[2], Departments of Chemistry and Biochemistry[1] and of Chemical Engineering[2], University of Colorado, Boulder, CO 80309

While numerous biological processes utilize membranes that contain transporting agents (carriers) to separate molecular and ionic permeates, the potential of synthetic membranes for separations in commercial processes has not been fully realized. In principal, the phenomenon of facilitated transport (FT) in membranes, which relies on the reversible formation of a permeate:carrier complex, can provide selective and efficient separations. Recently, membranes and thin films derived from ion exchange materials have received considerable attention with respect to their structural, physical and chemical properties. We report the facilitated transport of 1-hexene and 1,5-hexadiene between two decane phases separated by thin, hydrated membranes (ca. 25 μm). The flux of olefin across the membranes is enhanced by factors of several hundred when silver ions are exchanged for sodium ions.

Flux measurements were made using a two compartment cell arranged vertically and separated by the membrane which was held in place with o-rings and a clamp. The surface area of the membranes exposed to the solution was 1.8 cm^2. Both compartments of the cell contained decane (20 mL) that had been saturated with water and were mechanically stirred to provide efficient mass transport to and from the membrane. The lower compartment contained either 1-hexene or 1,5-hexadiene (0.1 M). After the cell was assembled, aliquots (1 μL) of the solution were removed periodically with a syringe from the upper compartment and injected into a gas chromatograph. The GC response for the olefins was monitored continuously by the injection of standards.

For membranes in the Na^+-form, the flux of olefin across the membrane was quite low, but stable for over two days. Transport rates were much higher for the membranes in the Ag^+-form. In both cases, plots of concentration of olefin in the upper compartment vs. time were linear. This indicates a constant flux of olefin across the membrane which can be readily calculated from the slopes: $J_{Na+,hexene} = 2.4 \times 10^{-13}$, $J_{Ag+,hexene} = 1.1 \times 10^{-10}$, $J_{Na+,hexadiene} = 4.0 \times 10^{-13}$ and $J_{Ag+,hexadiene} = 1.8 \times 10^{-10}$ (all J's in mol cm^{-2} sec^{-1}).

We attribute the enhanced olefin flux for the Ag^+-form of the membrane to the reversible complexation of the olefins with silver ion:

$$Ag^+ + \text{olefin} \rightleftharpoons Ag(\text{olefin})^+.$$

Formation constants for these complexes have been reported for 1-hexene ($K = 860$ M^{-1}) and 1,5-hexadiene ($K = 1850$ M^{-1}) in 1 M aqueous $AgNO_3$. Assuming that the enhanced fluxes are due to facilitated transport associated with the mobility of the $Ag(olefin)^+$ complex, facilitation factors, F, can be calculated as the ratio of the olefin flux for the Ag^+-form to the flux for the Na^+-form. From the fluxes calculated above, $F_{hexene} = 460$ and $F_{hexadiene} = 450$.

Synthetic fuels derived from coal liquids, tar sands or oil shale contain a wide variety of nonvolatile chemical compounds containing nitrogen and sulfur. Many of these compounds display mutagenic or carcinogenic activity. Therefore, these classes of compounds are undesirable pollutants which must be removed from fuels and other related hydrocarbon products.

We are exploring a novel process for the selective removal of organic nitrogen and sulfur compounds (R-N and R-S) from hydrocarbon phases. The process is based on electrochemically modulated chemical complexation. The complexing agents are water-soluble derivatives of Fe metalloporphyrins. A porphyrin (P) is a tetradentate macrocyclic ligand. Metalloporphyrins have numerous biological functions including the transport of oxygen. The metal ions in metalloporphyrins bind other molecules (ligands) in addition to the porphyrin itself. These bonds are perpendicular to the plane of the porphyrin so the bound molecules are referred to as axial ligands. Reversible reactions between metalloporphyrins and organic compounds containing nitrogen and sulfur are the basis for this separation process. In general, these complexation reactions have greater equilibrium constants when the metals are in the +2 oxidation state as opposed to the +3 state. Interconversion of the Fe(III) and Fe(II) states in metalloporphyrins is a kinetically facile process at metal electrodes. By applying relatively mild potentials, we can achieve the cyclical process:

cathode: $\mathrm{Fe(III)P} + e \longrightarrow \mathrm{Fe(II)P}$

$\mathrm{Fe(II)P} + \text{R-N or R-S} \longrightarrow \mathrm{Fe(II)P(RN\ or\ RS)}_{1\ \mathrm{or}\ 2}$

anode: $\mathrm{Fe(II)P(RN\ or\ RS)}_{1\ \mathrm{or}\ 2} \longrightarrow \mathrm{Fe(III)P} + e^- + \text{R-N or R-S}$.

The reactions described above can be incorporated into a staged electrochemical separation process. Results for the removal of isoquinoline and pentamethyene sulfide from iso-octane and the subsequent concentration of these compounds is a second (waste) hydrocarbon phase will be presented.

REMOVAL OF HYDROGEN CHLORIDE FROM HIGH TEMPERATURE COAL GASES

Gopala N. Krishnan, Bernard J. Wood, and Gilbert T. Tong

SRI International
333 Ravenswood avenue, Menlo Park, CA 94025

Vijendra P. Kothari

U.S. Department of Energy, Morgantown Energy Technology Center
3600 Collins Ferry Road, Morgantown, WV 26505

Introduction

The chlorine content of U.S. coals ranges from 0.01 to 0.5%, and some coals in U.K. contain as high as 1.0% chlorine.[1] This element is present in the coal mainly as alkali chlorides, but it also occurs as oxychlorides of calcium and magnesium.[2] During coal gasification or combustion, these chloride species are converted to HCl vapor. Concentrations of HCl vapor in coal gas have been found in the range 1 to 500 ppm.[3] The presence of HCl in the coal gas can lead to corrosion of metallic and ceramic components of the gasifier, attack gas turbine components and to poisoning of molten carbonate fuel cell electrodes.

Morgantown Energy Technology Center, as the U.S. Department of Energy's lead center for coal gasification and gas stream cleanup technology, has been concerned for some years with the purification of coal-derived gases for a range of applications including gas turbine, fuel-cell, and combined-cycle power generation. Removal of harmful impurities from the coal gas stream at elevated temperatures (>500°C) is necessary for achieving high thermal efficiency in such applications. Although the tolerance to HCl level of fuel cells has not been determined accurately, it is typical to specify that fuel cell feedstocks should contain no more than 1 ppm HCl. Similar requirements may be necessary in turbine applications. Currently available processes for removing HCl vapor operate at relatively low temperatures ($T < 300°C$) and thus they are not suitable for use with hot coal gases ($T > 500°C$). This paper presents the results of a laboratory-scale evaluation conducted at SRI International to determine the effectiveness of naturally occurring minerals and commercially available sorbents to remove HCl vapor from simulated coal gas streams at temperatures from 550° to 650°C.[4]

The thermodynamic stability and the volatility of the solid chloride products were the major criteria in selecting the nature of the sorbent. Alkaline earth chlorides, generally, are less volatile than alkali metal chlorides and transition metal chlorides. However, the calculated equilibrium partial pressure of HCl over alkali metal chlorides were calculated to be lower than those over alkaline earth compounds (Table 1). In considering these two factors, along with availability in a natural form, sodium carbonate based sorbents were judged to be superior to other compounds.

Table 1

EQUILIBRIUM PARTIAL PRESSURES OF HCl AND METAL CHLORIDES
AT 900 K IN PRESENCE OF A SIMULATED COAL GAS

Parent Compound	Product chloride (MCl)	Equilibrium Partial Pressure (atm)	
		HCl	MCl
Na_2CO_3	NaCl	1.5×10^{-6}	3.5×10^{-6}
K_2CO_3	KCl	3.0×10^{-6}	8.0×10^{-6}
$BaCO_3$	$BaCl_2$	2.2×10^{-5}	1.5×10^{-11}
$CaCO_3$	$CaCl_2$	9.5×10^{-4}	2.8×10^{-9}
$SrCO_3$	$SrCl_2$	1.5×10^{-4}	2.2×10^{-11}

Materials, Apparatus, and Experimental Procedures

Three naturally occurring minerals and a commercially available sorbent were selected for evaluation. The tested minerals were nahcolite ($NaHCO_3$), shortite ($Na_2CO_3 \cdot 2CaCO_3$), and dawsonite ($NaAl(OH)_2CO_3$). The mineral samples were pelletized and calcined at 600°C. During calcination the minerals decomposed as follows:

$$2\ NaHCO_3 \rightarrow Na_2CO_3 + H_2O + CO_2$$

$$Na_2CO_3 \cdot 2CaCO_3 \rightarrow Na_2CO_3 \cdot CaCO_3 + CaCO_3$$

$$NaAl(OH)_2CO_3 \rightarrow NaAlO_2 + CO_2 + H_2O$$

The natural minerals are characterized by low specific surface areas and high levels of active sodium components (Table 2). The commercial sorbent was Katalco Chloride Guard 59-3, manufactured by Katalco Corporation, Oakbrook, IL. This product is sold to remove chloride vapor from natural gas and light hydrocarbon feedstocks. The sorbent contains a proprietary active sodium compound impregnated on a porous alumina support and shows a very high specific surface area with a low level of active sodium component.

Table 2

PROPERTIES OF SORBENTS

Sorbent	Bulk density ($g.cm^{-3}$)	Surface area ($m^2 \cdot g^{-1}$)	ASC[1] (wt% Na)
Katalco Chloride Guard 59-3	0.76	247.0	4.7
Shortite	1.46	0.25	15.0
Nahcolite	0.65	1.2	40.3
Dawsonite	0.59	2.3	16.5

[1] ASC = Active sodium component expressed as wt% sodium.

The reactivities of the selected sorbents toward HCl vapor were evaluated in a thin bed, microreactor (Figure 1) under isothermal conditions. A simulated coal gas of composition 22% H_2, 34% CO, 7% CO_2, 36% H_2O, 1% He and 300 ppm HCl was used as a feedstock. The gas mixture was prepared by metering and blending the individual components using mass flow controllers. Glass or PTFE tubing was used to minimize adsorption or interaction of HCl vapor on the tube walls. Glass walls exposed to the HCl stream containing steam was kept heated to 180°C. The gaseous effluent leaving the sorbent bed was analyzed for HCl by reacting it with a 0.5 M $NaHCO_3$ buffer solution and measuring the dissolved $[Cl^-]$ with a chloride ion selective electrode. The cumulative concentration of the $[Cl^-]$ was calculated using the Nernst equation and the instantaneous partial pressure of HCl vapor in the reactor effluent was calculated by differentiating the cumulative chloride concentration with respect to time.

Results and Discussion

The reaction of the sorbent with HCl vapor yielded solid NaCl as the product:

$$Na_2CO_3 + HCl \rightarrow 2NaCl + CO_2 + H_2O$$

The rate of reaction with the sorbents was rapid initially, but it decreased with time onstream. Even at a space velocity of 5 x 10^4 h^{-1}, initial residual HCl vapor levels of about 1 ppm were attained with all the tested sorbents (Figure 2). The rate of removal of HCl and the chloride uptake capacity of the sorbents were found to be a functions of the level of its active sodium component (ASC) and its surface area (Table 3). Calcined nahcolite and dawsonite, with their high ASCs and moderate surface

Table 3

CHLORIDE UPTAKE CAPACITIES OF THE TESTED SORBENTS

Sorbent	Chloride capacity (wt%) 525°C	Chloride capacity (wt%) 650°C
Katalco Chloride Guard	7.1	4.3
Shortite	4.4	4.6
Nahcolite	52.5	52.5
Dawsonite	21.9	18.0

areas had high chloride uptake capacities. The chloride capacity of shortite was the smallest of the sorbents tested because of its low surface area in spite of its high ASC level. The capacity of Katalco Chloride Guard 59-3 was limited by the ASC level, although its surface area was very high.

In the range of 525° to 650°C, the temperature had only a small effect on the rate of HCl removal by shortite and nahcolite. Similarly, their maximum chloride uptake capacities were not affected by temperature. However, for Katalco Chloride Guard and dawsonite the uptake capacity at 650°C was less than at 530°C. Since these sorbents contain alumina, it is likely that at 650°C, the interaction of the active sodium component with the alumina present in the sorbent decreased their reactivity with HCl vapor.

Under the experimental conditions used, with very high surface area sorbents such as Katalco Chloride Guard, the rate of chloride uptake was controlled initially by gas phase mass transfer. Mass transfer calculations indicated that the rate of HCl vapor transfer from the gas phase (300 ppm) to the surface of Katalco Chloride Guard sorbent at 525°C would be about 2×10^{-6} $\text{mole}\cdot\text{g}^{-1}\cdot\text{s}^{-1}$ which compared favorably with the measured initial rate of 1×10^{-6} $\text{mole}\cdot\text{g}^{-1}\cdot\text{s}^{-1}$ at that temperature. At longer exposures, the rate became limited by pore diffusion. Effectiveness factor calculations indicated that pore diffusion could control the rate of chloride uptake with Katalco Chloride Guard once the external areas have been reacted. This rate limitation was confirmed when larger particles were found to react more slowly than smaller particles[4] in the size range of 0.05 to 0.5 cm. Rate control by other mechanisms such as chemical reaction at the interface or diffusion through the chloride product layer became predominant only when the sorbent was nearly saturated.

To determine the rate control mechanism with moderate surface area sorbents such as nahcolite, small quantities (0.1 g) of nahcolite were exposed to the gas mixture at a space velocity of 1 x 10^5 h^{-1} for various periods of time and the accumulated chloride in the solid was measured. Because of the small quantity of the sorbent and the large flow rate, the concentration of HCl vapor and the composition of the sorbent across the bed could be assumed to be nearly constant. The results of these experiments indicated that the rate of HCl reaction with nahcolite was limited initially by mass transfer. However, beyond an initial period, chemical reaction at the interface controlled the rate through a major portion of the sorbent active life time as indicated by a linear correlation between the log of the unreacted fraction (1-x) of the sorbent and time (Figure 3). This behavior is to be expected because of the relatively fewer number of micropores in a moderate surface area material in comparison with a high surface area material. Hence, the shift from mass transfer limited rate to chemical reaction limited rate would occur earlier with nahcolite than with Katalco Chloride Guard. After about 80% of the nahcolite sorbent has been reacted, the rate control appears to be limited by diffusion through a chloride product layer as indicated by the non linear behavior in log (1-x) vs. time plot.

Bench-scale experiments were also conducted with these sorbents at the Institute of Gas Technology, Chicago, IL.[5] The rate of chloride uptake was calculated from the analysis of the chloride content of the spent sorbent as a function of the bed depth. The results of bench-scale experiments were in general agreement with the laboratory-scale experiments although the HCl removal rate and the chloride capacities were somewhat lower than found in the laboratory-scale experiments. This may be due to the large particles used in the bench-scale study. Impurities such as H_2S and trace metals did not affect significantly the rate of HCl removal or the chloride capacities of the sorbents.

A preliminary economic analysis was performed at SRI to determine the cost of HCl removal from hot coal gas.[4] The cost of using Katalco Chloride Guard was estimated to be too high (~$0.02/kWh) for use as throwaway sorbent. In contrast, the annual operating cost for the use of nahcolite was estimated to vary from $0.0017 to $0.0031/kWh depending on whether the gasifier is oxygen-blown or air-blown. In this annual operating cost, the capital investment and the capital recovery components are major cost factors whereas the cost of nahcolite sorbent and its chloride capacity have only a small impact.

Conclusions

The reaction of HCl vapor with calcined sodium-carbonate based natural minerals and synthetic sorbents is rapid and the HCl vapor concentration can be reduced to about 1 ppm level in coal gas in the temperature range of 525° to 650°C. The rate of reaction is controlled initially by the rate of mass transfer from the gas phase to the surface of the sorbents. At later times the rate is controlled by diffusion through micropores in high surface area sorbents and by chemical reaction in moderate and low surface area sorbents. The presence of H_2S and trace metal impurities did not affect significantly the performance of the sorbents. The cost of HCl removal using naturally occurring mineral, nahcolite, is very low.

Acknowledgment

The authors wish to acknowledge the U.S. Department of Energy, Morgantown Energy Technology Center for support of this work under contract No. DOE-AC21-84MC21167.

References

1. W. H. Ode, "Coal Analysis and Mineral Matter" in *Chemistry of Coal Utilization*, supplementary volume, edited by H.H. Lowry, John Wiley and Sons, New York (1963).

2. T. L. Iapalucci, R. J. Demski, and D. Bienstock, "Chlorine in Coal Combustion", Reports of Investigation No. 7260, U.S. Bureau of Mines, (May 1969).

3. TRW, "Monitoring Contaminants in Coal Derived Gas for Molten Carbonate Fuel Cells", Final Report to Argonne National Laboratory under contract No. 31-109-38-6108, DOE/METC/82-44 (May 1981).

4. G. N. Krishnan, G. T. Tong, B. J. Wood, and N. Korens, "High Temperature Coal Gas Chloride Cleanup for Molten Carbonate Fuel Cell Applications", Report No. DOE/MC21167-2080 (November 1986).

5 G. L. Anderson and F. O. Berry, "Chlorine Removal from Hot Coal Gas," Report to SRI International by Institute of Gas Technology under contract No. C-11317 (April 1986). (see Appendix C of Reference 4).

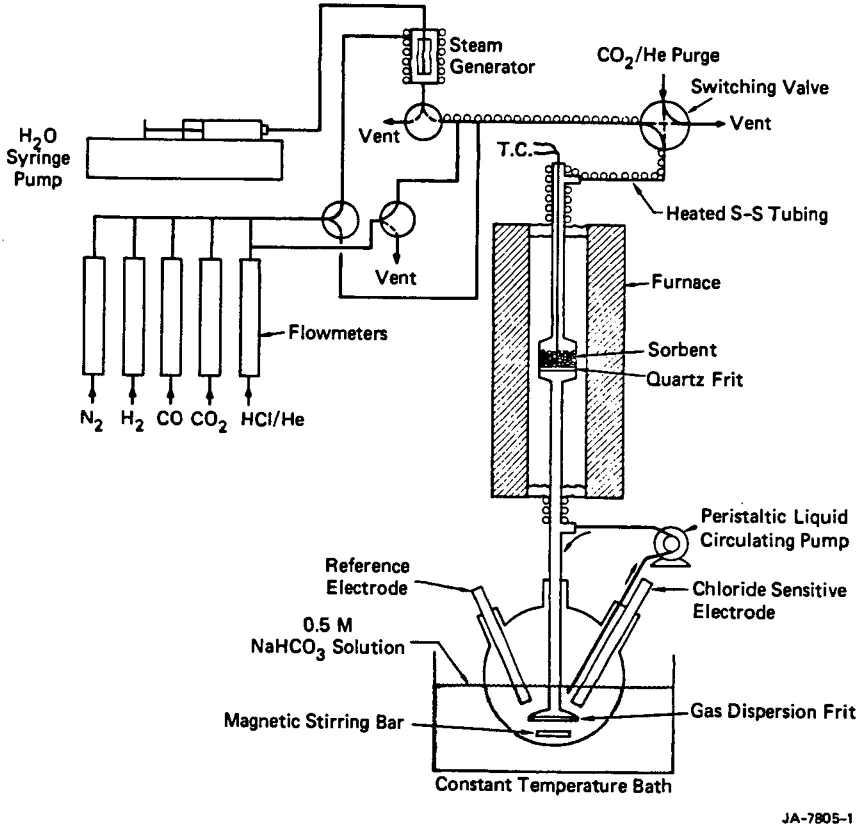
Steam
Generator
CO_2/He Purge
Switching Valve
Vent
Vent
H_2O
Syringe
Pump
T.C.
Heated S-S Tubing
Vent
Furnace
Flowmeters
Sorbent
Quartz Frit
N_2 H_2 CO CO_2 HCl/He
Peristaltic Liquid
Circulating Pump
Reference
Electrode
Chloride Sensitive
Electrode
0.5 M
$NaHCO_3$ Solution
Magnetic Stirring Bar
Gas Dispersion Frit
Constant Temperature Bath
JA-7805-1

Figure 1. Schematic diagram of thin bed reactor for studying HCl removal.

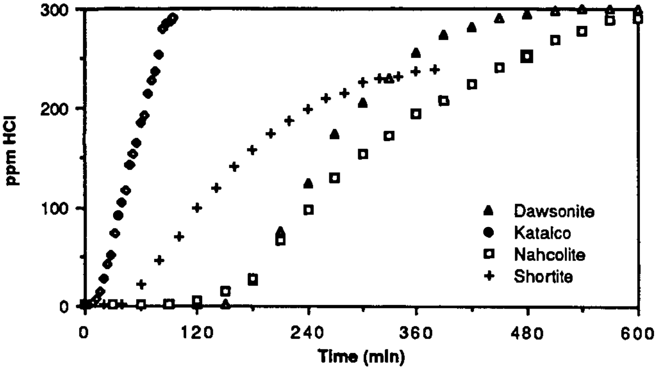

Figure 2. Examples of HCl Breakthrough Curves for Various Sorbents at 525°C
Sorbent quantity - Dawsonite = 0.4 g; Nahcolite = 0.2 g
- Katalco = 0.23 g; Shortite = 1.0 g

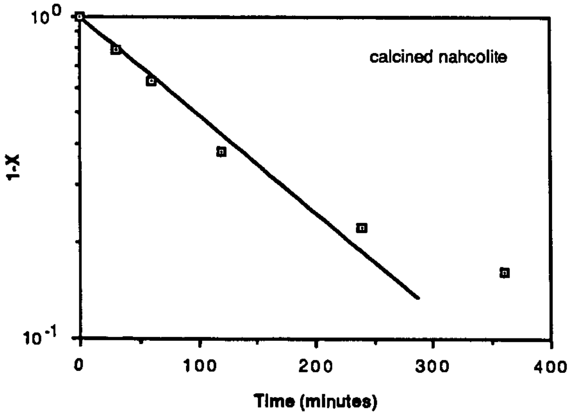

Figure 3 Plot of logarithm of unreacted fraction with time

REMOVAL OF H_2S FROM COAL-DERIVED GASES

by

S. Lynn, R.M. Hix, D.W. Neumann, S.F. Sciamanna, and C.A. Stevens
Department of Chemical Engineering
University of California, Berkeley, CA 94720

Introduction

When coal is gasified most of the sulfur is converted to H_2S and must be removed before the gas can be used either as a fuel or as synthesis gas. The UCB Sulfur Recovery Process (UCBSRP) is being developed as a general method for removing H_2S from gases. The H_2S is absorbed in a polyglycol ether, then reacted in the liquid phase with SO_2 to form marketable elemental sulfur and water. The process allows high specificity and flexibility; H_2S can be reduced to the part-per-million level or below in the presence of CO_2 and the other components of gasified coal. The CO_2 may be left in the original gas stream or it may be co-absorbed and recovered as a separate, sulfur-free product. The process thus has application both to syngas and hydrogen production from O_2-blown gasifiers and to power production using an air-blown gasifier.

Process Configurations

Figure 1 shows a flowsheet for the UCBSRP in a configuration that gives maximum selectivity for H_2S removal. In the primary absorber H_2S is removed primarily by physical absorption. The stream of solvent leaving the absorber is nearly saturated with all of the components of the gas being treated. A water wash at the top of the primary absorber prevents loss of solvent vapor in the treated gas.

Most of the solvent stream leaving the primary absorber then enters a reactor/crystallizer that operates at the pressure of the primary absorber. A second solvent stream containing SO_2 is metered into the same reactor at a rate that keeps the SO_2 content within the reactor a few percent above stoichiometric relative to the H_2S. (It is necessary to have an excess of one reactant or the other in each reactor to avoid excessive reactor volumes and the need for highly precise reactor control.) A clarified overflow from the SO_2-rich reactor is pumped back to the primary absorber. This solvent stream has been completely freed of its H_2S content but is still saturated with respect to the other components in the gas being treated in the primary absorber. The net co-absorption of these other gas components (such as CO_2) is thus kept quite small and the effective selectivity for H_2S is of the order of 50 to 100. The SO_2 content of this solvent stream, although low, provides a chemical enhancement for the absorption of the H_2S on the upper trays of the primary absorber to facillitate meeting very stringent H_2S specifications in the treated gas. (The temperature in the primary absorber is high enough to prevent precipitation of the sulfur formed by this reaction. Not shown in

- - - - -

For presentation at the symposium "Separation Processes for Coal Conversion"
Toronto Meeting, American Chemical Society, June, 1988.

Figure 1, to avoid clutter, is provision for cooling both reactor/crystallizers with cooling water so that the solvent is sub-saturated in sulfur at all other points in the system.)

The underflow from the SO_2-rich reactor carries the sulfur and water formed in the reaction between H_2S and SO_2. The flow of this stream is sized to keep the water content of the solvent from exceeding 5% and is directly proportional to the rate of H_2S removal - - the flow will typically be about 10% of the total flow of solvent through the primary absorber. Sufficient H_2S-rich solvent, from the primary absorber, is added to the stream to leave a small excess of H_2S after all of the residual SO_2 has reacted. This stream is then flashed to atmospheric pressure in the settler/surge tank.

The sulfur made in the process forms a slurry in the underflow from the surge tank. The sulfur is recovered and washed in a centrifuge. In most cases about one-third of the sulfur will be burned in the furnace to make the SO_2 needed in the process. The energy recovered in the waste-heat boiler will usually supply and perhaps exceed the energy required by the process.

The overflow streams from the surge tank and the centrifuge are combined and sent to the solvent stripper. Boiling most of the water out of the solvent provides a stripping vapor that also removes unreacted H_2S and co-absorbed gases such as CO_2 from the solvent. Most of the solvent leaving the solvent stripper is used in the SO_2 scrubber where it absorbs the SO_2 from the combustion gas leaving the furnace. The SO_2 content of this solvent is nil, and hence the SO_2 content of the stack gas leaving the scrubber can readily be reduced to the part-per-million level. The remainder of the solvent from the stripper is sent to the primary absorber, where it prevents loss of SO_2 in the treated gas.

Figure 2 shows a process configuration suitable for removing and recovering one or more components (in addition to the H_2S) from the gas being treated, such as removing CO_2 from a synthesis gas ahead of a shift reactor in a process for producing hydrogen. The operation of this process is identical to that described above in many respects. It differs as follows:

At the bottom of the primary absorber is a short section in which much of the H_2 and CO are stripped from the solvent. The stripping gas is obtained by a partial flash of the solvent immediately downstream of the primary absorber. Most of the H_2S-rich solvent stream leaving the flash drum, together with a controlled flow of SO_2 solution, enters an SO_2-rich reactor. The pressure of the SO_2-rich solvent stream is reduced in stages (only two are shown) to about one atmosphere. The off-gas from each stage is recompressed to the pressure desired for the CO_2 product and is contacted with neat solvent to remove traces of SO_2, then washed with water to recover solvent vapor. For the case shown, in which a high degree of CO_2 removal is not required, clarified H_2S-free solvent from the atmospheric flash can be pumped directly back to the primary absorber.

As in the flow configuration designed for high H_2S selectivity, the sulfur and water formed in the reaction are conveyed out of the last SO_2-rich reactor in a stream that is rendered H_2S-rich with by-passed H_2S solution. As before, the flow of this stream is proportional to the rate of sulfur production.

Lynn, et al. (1987) compared conventional technology to the UCBSRP for removing H_2S from the recycle gas of a crude oil residuum hydrodesulfurization unit. The UCBSRP has the potential for significantly reducing both the capital and operating costs because of the reduction in the number of processing steps and in utilities consumption. Lynn and Sciamanna (1988c) found a similar advantage for the UCBSRP for treating natural gas to remove H_2S, water and C_{3+} hydrocarbons.

Gas and Sulfur Solubilities in Process Solvents

The solubilities of H_2S, SO_2, CO_2, propane, butane and sulfur in a variety of glycol ethers have been measured as a function of temperature. Water, a product of the reaction, reduces these solubilities. These results have been reported by Demyanovich and Lynn (1987) and by Sciamanna and Lynn (1988a and 1988b).

Reaction Kinetics

The reaction between H_2S and SO_2 in glycol ethers is relatively slow when uncatalyzed. However, as reported by Neumann and Lynn (1986), tertiary aromatic amines are effective catalysts and reduce the time required for nearly complete reaction to a few seconds.

Corrosion Studies

Corrosion studies were performed by submerging metal coupons half way in a solution of H_2S or SO_2 in a glycol ether. To make the system as corrosive as possible, the solvent was a mono-ether (which is also an alcohol) and sulfur and water were added in concentrations twice (or greater) those encountered in the process. The exposure was carried out for three successive 20 to 30-day periods at each temperature. Table 1 shows the corrosion rates observed.

Table 1: Corrosion Rates of Steels in Process Solutions.

	MEASURED RATES AND CONDITIONS *		
Metal	SO_2: @ 100°C	@ 120°C	H_2S: @ 150°C
Carbon Steel	0.6	1.7	0.05
304 Stainless	0.7	1.5	0.02
316 Stainless	1.3	4.8	0.01

* Mils/year in diethylene glycol methyl ether, 5% H_2O, saturated with sulfur, 50 - 100 psi gas pressure.

Since 60°C is the maximum temperature at which SO_2 is present (outlet of the SO_2 absorber), carbon steel and 304 and 316 stainless steels should corrode at rates much less than 1 mil/year (0.02 mm/yr) under all process conditions.

Sulfur Crystallization

A major potential advantage of the UCB Sulfur Recovery Process is the purity of the crystalline sulfur that is produced. The sulfur crystallizes from solution both as a result of cooling and as a result of chemical reaction between H_2S and SO_2. In the former case the degree of supersaturation is relatively low because the solubility of sulfur in the solvent varies only a few grams per liter over the temperature range of interest. A substantially higher concentration of sulfur can result from the chemical reaction.

The crystallizer consists of a well-stirred 2-liter vessel. Hot saturated feed enters at the top, and the vessel walls are cooled. Cold effluent exits at the bottom of the vessel as a sulfur/solvent slurry. A sample of the effluent slurry is collected when the system is at steady-state and the size distribution of the sulfur crystals is determined. analysis.

Gas Absorption with Chemical Reaction

Tray efficiency data are needed for two process situations. In one, H_2S at very low concentration is being absorbed by a chemically reactive solution of SO_2. In the other, gaseous SO_2 in the low parts-per-million concentration range is absorbed by lean process solvent. Both are of interest because one wishes to effect very stringent sulfur removal with the UCBSRP. The equipment consists of a single seive tray (or section of packed column) placed in a test section through which gas and liquid streams pass. Murphree tray efficiencies are determined from the mass balances and previously obtained solubility data.

Work Required for Proof-of-Concept

The crystallizer is being modified to incorporate crystal size classification to retain smaller crystals and produce a product of larger size. Sulfur will be produced by chemical reaction. Data obtained for absorption of H_2S enhanced by the presence of SO_2 in the solvent will be used to develop a model that incorporates the reaction kinetics work done previously.

A computer model that simulates all of the unit operations in the process is operational and facillitates process synthesis for specific applications. It will be used to evaluate and further refine the process configurations shown in Figures 1 and 2 for the purification of hydrogen derived from gasified coal.

Acknowledgement

This work was supported by the Assistant Secretary for Fossil Energy, Office of Coal Utilization, Division of Surface Coal Gasification, of the U.S. Department of Energy under contract DE-AC03-76SF00098.

References

Demyanovich, R.J. and Lynn, S. **1987**. Vapor-Liquid Equilibria of Sulfur Dioxide in Polar Organic Solvents. *I&EC Research* **26** 548.

Lynn, S., Neumann, D.W., Sciamanna, S.F., and Vorhis, F.H. 1987. A Comparison of the UCB Sulfur Recovery Process with Conventional Sulfur Recovery Technology. *Environmental Progress* 6 257.

Neumann, D.W. and Lynn, S. **1986**. Kinetics of the Reaction of H_2S and SO_2 in Organic Solvents. *I&EC Proc. Des. & Dev.* **25** 248.

Sciamanna, S.F. and S. Lynn, **1988**. Sulfur Solubility in Pure and Mixed Organic Solvents. *I. & E.C. Research* (in press).

Sciamanna, S.F. and S. Lynn, **1988**. Solubility of Hydrogen Sulfide, Sulfur Dioxide, Carbon Dioxide, Propane and n-Butane in Polyglycol Ethers. *I. & E.C. Research* (in press).

Sciamanna, S.F. and S. Lynn, **1988**. An Integrated Process for Simultaneous Desulfurization, Dehydration, and Recovery of Hydrocarbon Liquids from Natural Gas Streams. *I. & E.C. Research* (in press).

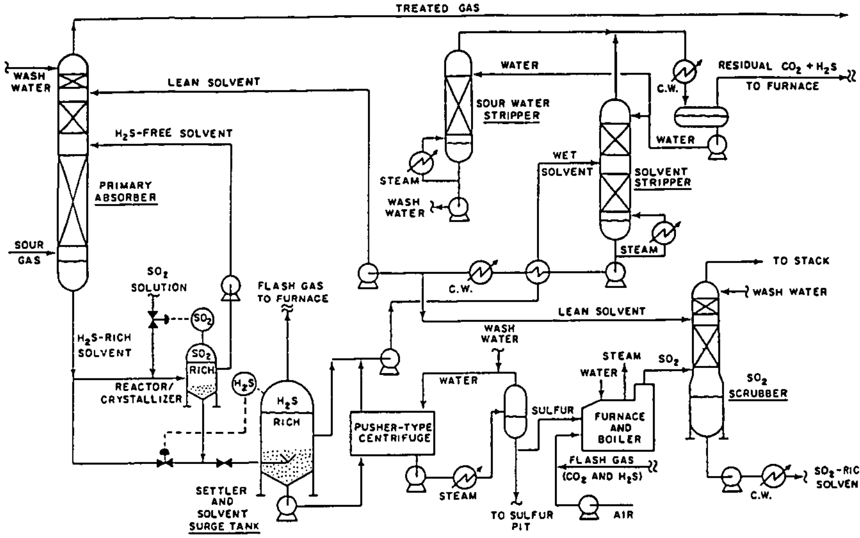
TREATED GAS
WASH WATER
LEAN SOLVENT
H2S-FREE SOLVENT
PRIMARY ABSORBER
SOUR GAS
SO2 SOLUTION
SO2
SO2 RICH
H2S-RICH SOLVENT
REACTOR/ CRYSTALLIZER
H2S
FLASH GAS TO FURNACE
H2S RICH
SETTLER AND SOLVENT SURGE TANK
PUSHER-TYPE CENTRIFUGE
STEAM
WATER
SOUR WATER STRIPPER
STEAM
WASH WATER
WET SOLVENT
SOLVENT STRIPPER
STEAM
C.W.
RESIDUAL CO2 + H2S TO FURNACE
WATER
C.W.
LEAN SOLVENT
WASH WATER
WATER
SULFUR
TO SULFUR PIT
STEAM
WATER
FURNACE AND BOILER
FLASH GAS (CO2 AND H2S)
AIR
SO2
TO STACK
WASH WATER
SO2 SCRUBBER
C.W.
SO2-RICH SOLVENT

Figure 1 H_2S-Selective Process.

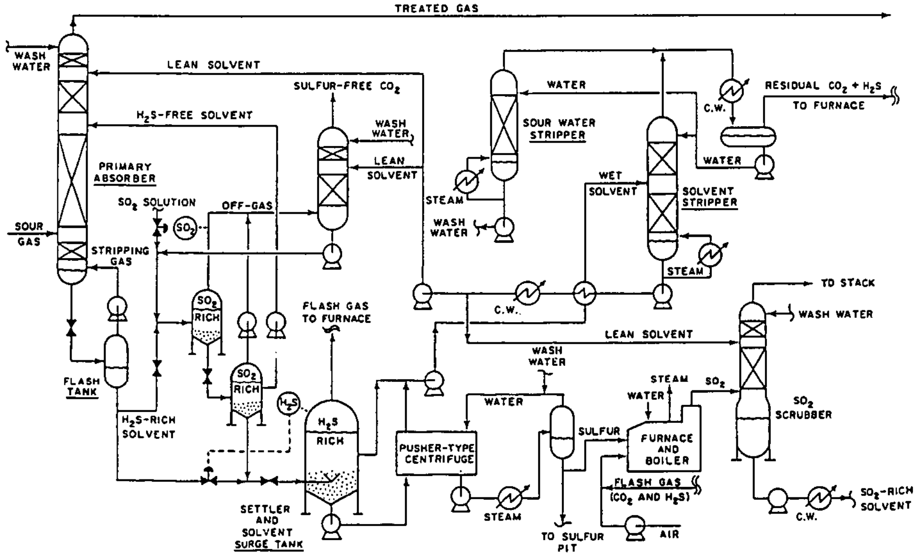
TREATED GAS
WASH WATER
LEAN SOLVENT
H2S-FREE SOLVENT
SULFUR-FREE CO2
WASH WATER
LEAN SOLVENT
PRIMARY ABSORBER
SO2 SOLUTION
SO2
OFF-GAS
SOUR GAS
STRIPPING GAS
FLASH TANK
H2S-RICH SOLVENT
SO2 RICH
SO2 RICH
H2S
FLASH GAS TO FURNACE
H2S RICH
SETTLER AND SOLVENT SURGE TANK
PUSHER-TYPE CENTRIFUGE
STEAM
WATER
SOUR WATER STRIPPER
STEAM
WASH WATER
WET SOLVENT
SOLVENT STRIPPER
STEAM
C.W.
RESIDUAL CO2 + H2S TO FURNACE
WATER
C.W.
LEAN SOLVENT
WASH WATER
WATER
SULFUR
TO SULFUR PIT
STEAM
WATER
FURNACE AND BOILER
FLASH GAS (CO2 AND H2S)
AIR
SO2
TO STACK
WASH WATER
SO2 SCRUBBER
C.W.
SO2-RICH SOLVENT

Figure 2 Co-Absorption Process.

SORBENT-BASED RECOVERY OF SULFUR FROM REGENERATION TAIL GASES

S. K. Gangwal and S. M. Harkins
Research Triangle Institute, Research Triangle Park, NC 27709

T. P. Dorchak, Morgantown Energy Technology Center, Morgantown, WV 26507

The U.S. Department of Energy (DOE), Morgantown Energy Technology Center (METC) is sponsoring research on advanced methods for controlling contaminants for hot coal gas streams of integrated gasification combined-cycle (IGCC) systems.(1) The programs focus on hot gas cleanup technologies that match or nearly match the temperatures and pressures of the gasifier, cleanup system, and power generator. The purpose is to eliminate the need for expensive heat recovery equipment and to avoid the efficiency losses associated with fuel gas quenching. DOE/METC has originated the Gasification Island concept for IGCC systems, which combines temperature and pressure matching, modular shop fabricated construction, and steam and air integration of the gasifier and turbine. Figure 1 illustrates the simplified IGCC system that can be achieved with hot gas cleanup. For the control of sulfur in the coal gasifier gas, DOE/METC continues to conduct and to sponsor work toward the development of a zinc ferrite absorption process. Absorption capacity of the zinc ferrite is highest at temperatures of 800 to 925 K compatible with the operation of a fixed-bed gasifier turbine system.

The hydrogen sulfide laden fuel gas passes through a fixed bed of zinc ferrite, in the form of 3/16-inch extrudates, which absorbs sulfur up to 25 percent of its weight. The clean gas contains less than 5 ppm, well below New Source Performance Standards (NSPS) and also enhances corrosion and erosion protection for the downstream turbine. The sulfided sorbent is regenerated with a dilute typically less than 2 percent oxygen containing gas. The oxygen content of the regenerator gas is limited to avoid overheating and sintering the sorbent due to the highly exothermic oxidation of the sulfide to sulfur dioxide. The tail gas from the regeneration process must be further processed to remove the sulfur and recover it in an environmentally acceptable manner in a salable or readily disposable form.

This paper will discuss the results of experimental/theoretical research on two novel process concepts for elemental sulfur production from regeneration tail gases. Both concepts utilize a highly efficient sodium/aluminum (Na/Al) based SO_2 sorbent at elevated temperatures (800 to 1,000 K) and pressures (1 to 3 MPa). One concept involves sulfation of the Na/Al sorbent with the tail gas followed by regeneration with reducing gas to produce a suitable Claus plant feed. The other concept aims for single step sulfur production by reacting the tail gas with a small quantity of raw coal gasifier product gases over the sorbent.

The first concept is schematically shown in Figure 2. The SO_2 in the tail gas is absorbed onto the Na/Al sorbent and the hot diluent is recycled for regenerating zinc ferrite. The sulfated Na/Al sorbent is then regenerated using a small side stream of the coal gasifier gas. The resulting concentrated sulfur stream at elevated temperature and pressure containing from 10 to 50 percent H_2S is a suitable feed for a Claus plant for elemental sulfur recovery.

The preparation of the Na/Al sorbent follows from Beinstock et al. at the U.S. Bureau of Mines for the removal of SO_2 from combustion flue gases.(2) Further development in this study has produced a sorbent as strong 1/16 inch to 1/8 inch extrudates with greater structural integrity, reactivity, capacity, and mechanical strength.(3) Enhancement of these properties is believed to be necessary for successful application at high temperature and pressure conditions.

The sorbent has been tested at atmospheric pressure as well as elevated pressures to demonstrate the potential of the concept shown in Figure 2. Atmospheric pressure tests have been carried out using both a fixed-bed reactor system and a thermogravimetric reactor (TGR) system. Tests have been conducted at 800 to 975 K with a tail gas containing 1 to 2 percent SO_2. These conditions are representative of zinc ferrite regeneration tail gas. Atmospheric pressure tests have shown that the sorbent can absorb SO_2 up to 40 percent of its weight. The sorbent can be regenerated while maintaining a crush strength greater than 13.5 N/mm over 20 sulfation/regeneration cycles. In atmospheric pressure fixed-bed tests, the sorbent demonstrated high efficiency in absorbing SO_2 by reducing it from 2 percent to less than 10 ppmv. This essentially "zero" prebreakthrough level of SO_2 was maintained for over 2 hours at a space velocity of 2000 h^{-1}. Approximately 30 percent by weight SO_2 was absorbed prior to 100 ppm SO_2 breakthrough. Regenerations of the sorbent with coal gasifier gas and hydrogen in separate tests produced H_2S rich gas streams containing up to 16.4 and 60 percent H_2S, respectively.

Elevated pressure TGR tests have recently been initiated to evaluate sulfation and regeneration kinetics that could be used to predict fixed-bed sorbent performance at elevated pressure. Figure 3 compares the atmospheric pressure sulfation rate to sulfation rate at 2.5 MPa. As can be seen, the overall SO_2 absorption capacity as a function of time is significantly higher at 2.5 MPa. This indicates that it will be possible to sulfate a fixed-bed of the sorbent to significantly greater levels at elevated pressures than at atmospheric pressure, prior to breakthrough. Following completion of measurement of elevated pressure sulfation/regeneration kinetics, a fixed-bed absorption/regeneration model will be developed to predict sorbent capacity at breakthrough in fixed-bed reactors. Bench-scale tests will then be carried out to demonstrate the concept at elevated pressures.

Elemental sulfur has been observed on the surface of the sorbent following sulfation/regeneration cycles. Also significant amounts of elemental sulfur elutes from the sorbent after breakthrough has been achieved during sulfation. This has suggested a second concept for direct recovery of elemental sulfur from regeneration tail gases which if successful would result in significant reduction of the burden on the Claus plant. Ideally this concept (shown schematically in Figure 4) may allow the complete elimination of the Claus plant. A thermodynamic analysis of potential sulfur forming reactions of H_2, SO_2, CO, H_2S, CO_2, and steam indicates that 96 to 98 percent of the SO_2 can be potentially converted to elemental sulfur at 800 to 1,000 K and 2.5 MPa. A few bench-scale tests will be carried out in the future to assess the potential of this concept.

References

1. U.S. Department of Energy, "Hot Gas Cleanup for Electric Power Generation Systems," Morgantown Energy Technology Center, DE86006607, May (1986).

2. Bienstock, D., J. H. Field, and J. G. Myers, Bureau of Mines, Department of Investigations, 5735, PB 192542 (1961).

3. Gangwal, S. K., S. M. Harkins, and M. C. Woods, "Disposal of Off-Gases from Hot Gas Desulfurization Processes," Yearly Technical Status Report, Contract No. DE-AC21-86MC 23260, to be published (1987).

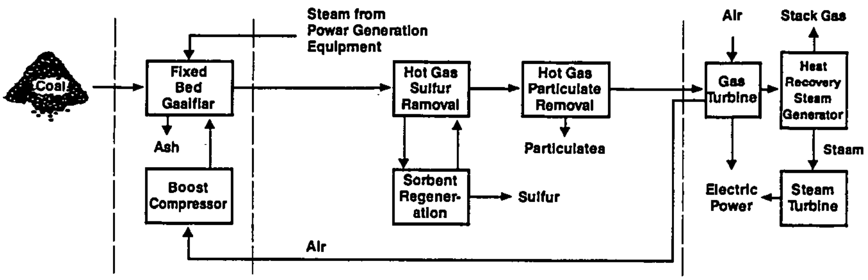
Coal
Fixed Bed Gasifier
Ash
Boost Compressor
Steam from Power Generation Equipment
Hot Gas Sulfur Removal
Sorbent Regeneration
Sulfur
Hot Gas Particulate Removal
Particulates
Air
Gas Turbine
Air
Stack Gas
Heat Recovery Steam Generator
Steam
Electric Power
Steam Turbine

Figure 1. Gasification island concept for IGCC systems.

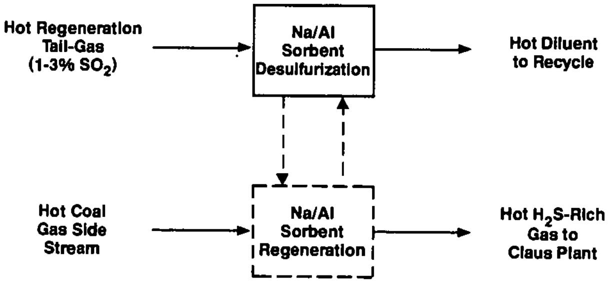
Hot Regeneration Tail-Gas (1-3% SO_2)
Na/Al Sorbent Desulfurization
Hot Diluent to Recycle
Hot Coal Gas Side Stream
Na/Al Sorbent Regeneration
Hot H_2S-Rich Gas to Claus Plant

Figure 2. High temperature regeneration tail-gas treatment.

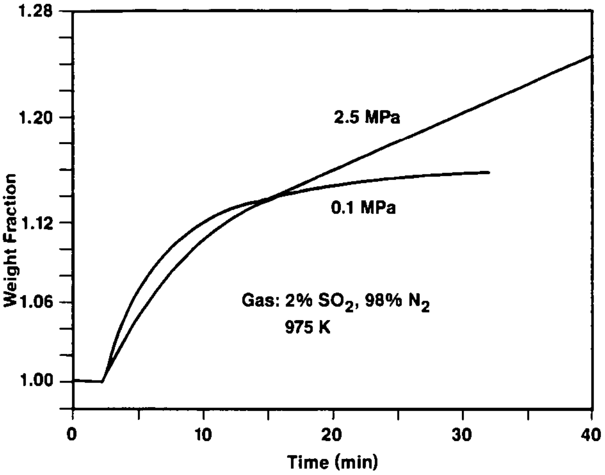

Figure 3. Effect of pressure on sorbent sulfation rate.

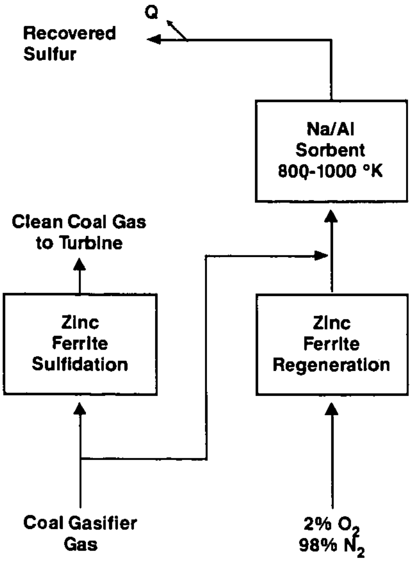
Q
Recovered Sulfur
Na/Al Sorbent 800-1000 °K
Clean Coal Gas to Turbine
Zinc Ferrite Sulfidation
Zinc Ferrite Regeneration
Coal Gasifier Gas
2% O_2
98% N_2

Figure 4. Direct recovery of sulfur from regeneration tail-gas.

SEPARATION OF GAS MIXTURES BY TRANSITION-METAL COMPLEXES

M. A. Lilga, R. T. Hallen, D. A. Nelson

Battelle, Pacific Northwest Laboratory
P.O. Box 999
Richland, WA 99352

INTRODUCTION

The selective separation or purification of gases, especially hydrogen and CO, is highly desirable in processes utilizing product gas from coal gasification. However, gas separation is a difficult and energy intensive process. The development of new and innovative methodologies to selectively and efficiently separate specific gas components from mixed-gas streams would significantly reduce the cost and complexity of product gas production and processing. For example, efficient H_2 separation from synthesis gas could make coal an attractive future source of H_2 for use as a fuel or chemical feedstock. In addition, this technology could have a significant impact on processes not directly associated with coal gasification in which hydrogen is lost in a waste stream. These processes include ammonia manufacture, reduction of metallic oxide ores, and hydrogenation of fats and oils. Thus, wide-ranging applications exist for hydrogen separation and recovery technologies.

Current separation technologies are inefficient or non-selective. For example, recovery of H_2 from Pressure Swing Adsorption is on the order of 80%. PSA is ineffective with feeds containing less than 50% H_2. The COSORB^{TM} process for CO recovery is highly moisture sensitive, requiring removal of water from feed streams. Membranes are inherently energy efficient but systems, such as PRISM^{TM}, cannot separate H_2 from CO_2.

The Pacific Northwest Laboratory (PNL) is examining transition-metal complexes as selective agents for the separation of syngas components from gas mixtures. Transition-metal complexes are known which react reversibly with gases such as H_2, CO, O_2, and CO_2. This reversible binding can be used to transfer the gas from a region of high partial pressure to a region of lower partial pressure. The selectivity of transfer is determined primarily by the selectivity of the metal in binding a specific gas. The nature of the ligands surrounding the metal has a large influence on the selectivity and reversibility and we have successfully used ligand modification to prepare complexes that have improved properties for H_2 or CO binding. Applications of metal complexes to gas separation and two specific examples of metal complexes under study will be discussed.

APPLICATION OF METAL COMPLEXES TO GAS SEPARATION

Two gas separation systems which take advantage of selective, reversible gas binding by transition-metal complexes are absorption/desorption and facilitated transport membrane systems. A two-column apparatus used at PNL is shown in Figure 1 and its operation is illustrated for CO separation. Inlet gas containing CO enters the bottom of the absorber column and encounters a counter-current flow of solution containing a metal complex. Non-reactive feed gases exit the top of the absorber while CO is transported to the stripper column in the form of a CO/metal complex. Heat and an inert stripping gas release the CO from the metal complex in the stripper column. CO product gas exits the top of the stripper column and volatilized solvent is condensed and returned to the system. The solution containing regenerated metal complex is recycled to the top of the absorber column and the cycle begins again. This apparatus is similar to that used in the COSORB^{TM} process and allows for continuous gas separation. Any gas could be separated from a feed stream by this process assuming an appropriate metal complex/solvent system specific for that gas is available. Potential drawbacks include the relatively large amounts of carrier required and the interference of solubility of undesired gases in the solvent.

Immobilized liquid membrane systems, in which the metal complex acts as a facilitated transport agent, offer the potential for high selectivity and increased flux. This type of system is illustrated in Figure 2 for H_2 separation. The driving force to separation is a pressure gradient across the membrane. Hydrogen entering the membrane on the high pressure side reacts with a metal complex. The metal/hydrogen complex diffuses across the membrane where H_2 is released in the H_2-lean environment and product H_2 leaves the membrane and is removed. A concentration gradient drives the metal complex back across the membrane and more H_2 is bound the continue the cycle. The function of the metal complex is to act as a specific carrier for H_2 and serves to increase the effective H_2 concentration in the membrane relative to the undesired gases. Thus, selectivity for H_2 is high, allowing the use of thinner membranes resulting in a greater flux. Permeability and selectivity in these systems are expected to be significantly greater than for dry or liquid-wetted membranes.

PALLADIUM COMPLEXES

Palladium dimer complexes were evaluated for their ability to reversibly bind CO (Equation 1). Kinetic and thermodynamic data for these complexes (X = NCO, Cl, Br, I) indicate that halide substitution greatly influences the binding of CO (1). For example, the equilibrium constant, K, for CO binding follows the order NCO > Cl > Br > I where K for the NCO complex is approximately 300 times that of the iodide complex. This difference in equilibrium constant is primarily due to differences in k_{-1}, the rate of CO dissociation.

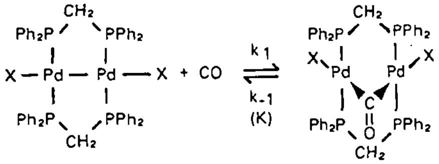

1)

Specificity for CO is high. Gases including CO_2, N_2, H_2, O_2 and ethylene do not interfere with CO binding. H_2S was found to react in a novel way to release H_2 according to Equation 2 (2).

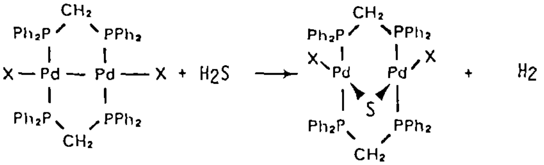

2)

Equilibrium data for the bromide complex indicated suitable reversibility over the temperature and CO pressure ranges of interest. This complex was chosen for bench-scale experiments in the absorber/stripper system shown in Figure 1 (3). Presence of the complex enhances transfer of CO by an order of magnitude and the system functions to separate CO from N_2. With a five-component mixture (CO, CO_2, H_2, CH_4, and N_2) a combination of chemical complexation of CO and the solubility of CO_2 and CH_4 in the solvent resulted in significant transfer of these gases to the stripper. Little H_2 was transferred and an H_2-rich gas stream was produced indicating the potential of this system for H_2 separation from a low-btu gas mixture. A cost analysis indicated that the initial costs of palladium were not necessarily prohibitive but to compete with existing technology the lifetime of the complex must be at least one year.

CHROMIUM COMPLEXES

The reaction of H_2 with $[CpCr(CO)_3]_2$ (Cp = cyclopentadienyl, C_5H_5) was reported by Fischer, et al. (4,5) to occur at 70°C and 150 atm H_2 to afford the monomeric hydride complex $CpCr(CO)_3H$. It has also been reported that the pure monomeric hydride complex evolves H_2 when heated to 80°C, its melting point. Our initial objective was to determine the temperature and H_2 pressure conditions required to carry out the reversible H_2 binding in solution (Equation 3).

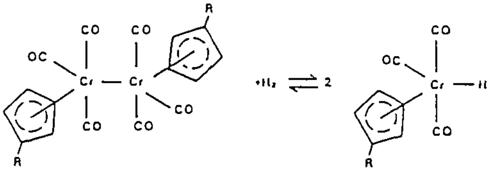

3)

Derivatives of the complex were also prepared to study the effects of electron-withdrawing groups on the cyclopentadienyl ligand (R = CO_2CH_3) on Equation 3. Our investigation has demonstrated that the reaction of H_2 with $[CpCr(CO)_3]_2$ is much more facile than previously reported. At 10 atm and room temperature, the reaction is complete before a spectrum can be taken. This dimer is found to react with 1 atm H_2 slowly at room temperature but faster at 65°C, reaching completion in 0.5 hours. Regeneration to the extent of about 5% can be achieved by heating to 100°C for 2 hours. H_2 is rapidly lost upon photolysis, however, CO is also lost and an inactive complex is formed. The substituted complex shows similar activity for H_2 binding but regeneration appeared to be easier with 10% conversion at 90°C after two hours. Regeneration may be difficult because it involves a bimolecular process in which two chromium centers interact. It is possible that regeneration will be improved by linking the cyclopentadienyl groups together, since hydrogen formation would then be unimolecular.

CONCLUSIONS

Selective transition-metal complexes can enhance gas transport in gas separation processes. Properties of complexes can be tailored by chemical modification of the ligand environment to improve binding characteristics. As a result, high selectivity for specific gas components is attainable. In addition, complexes need not be prohibitively expensive.

ACKNOWLEDGMENT

This research was supported by the U.S. Department of Energy, Morgantown Energy Technology Center under contract DE-AC06-76RLO 1830.

REFERENCES

(1) Lee, C. L.; James, B. R.; Nelson, D. A.; Hallen, R. T. *Organometallics*, 1984, *3*, 1360.

(2) James, B. R.; Lee, C. L.; Lilga, M. A.; Nelson, D. A. U.S. Patent 4 693 875, 1987.

(3) Lyke, S. E.; Lilga, M. A.; Ozanich, R. M.; Nelson, D. A. *Ind. Eng. Chem. Prod. Res. Dev.*, 1986, *25*, 517.

(4) Fischer, E. O. *Inorg. Synth.*, 1963, *7*, 136.

(5) Fischer, E. O.; Hafner, W.; Stahl, H. O. *Z. Anorg. Allgem. Chem.*, 1955, 282, 47.

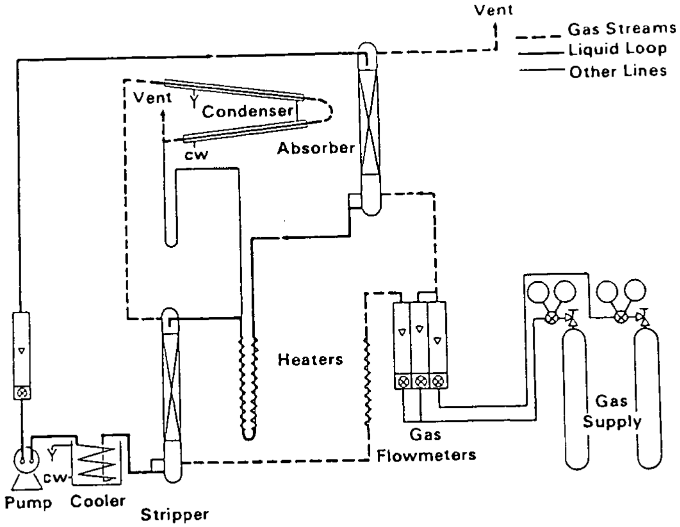
Vent
Gas Streams
Liquid Loop
Other Lines
Vent
Condenser
cw
Absorber
Heaters
Gas
Supply
Gas
Flowmeters
Pump
Cooler
cw
Stripper

FIGURE 1. Absorber/Stripper Apparatus

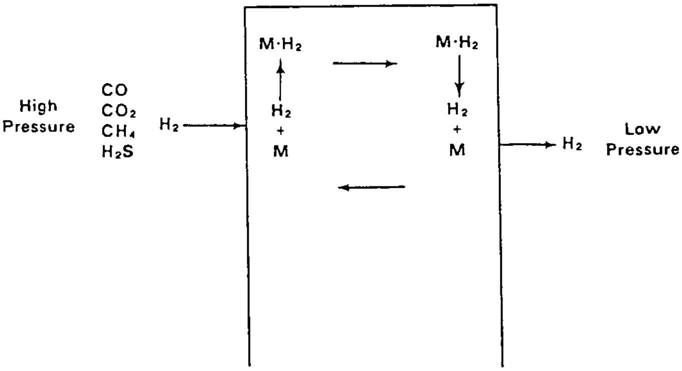
High
Pressure
CO
CO₂
CH₄
H₂S
H₂
M·H₂
H₂
+
M
M·H₂
H₂
+
M
H₂
Low
Pressure

FIGURE 2. Facilitated Transport of H_2 by a Membrane Containing a Dissolved Metal Complex

The Removal of Impurities from Hot Coal-Derived Gas by Filtration

by

T. Grindley and R. G. Logan
U.S. Department of Energy
Morgantown Energy Technology Center
Morgantown, WV 26505

At the Morgantown Energy Technology Center (METC) of the U.S. Department of Energy, an effort is underway to clean hot coal-derived gas to a sufficient purity for combustion in heat engines and other applications. Experiments were conducted in which the hot product gas, raw and desulfurized, from a fluid-bed coal gasifier was filtered at temperatures up to 1,600°F, pressures up to 250 psig, and flow rates up to 2,500 scfh. Particulate and condensate samples were collected at the inlet and outlet of the filters and analyzed for 10 metals which are common constituents of coal ash. The results were used to determine how filtration of particles from a gas stream at high temperatures affected metal concentrations in the gas. In general, the removal efficiency for the metals correlated with the particulate removal efficiency.

Introduction

Under the Advanced Environmental Control Technology Program established in 1979 by the Department of Energy (1), Morgantown Energy Technology Center has been actively engaged in the development of technology necessary to control contaminants from coal gasification that are deleterious to gas turbines and hazardous to the environment. A significant part of this effort has been concerned with particulate and trace metal, particularly alkali metals, removal from the hot gas streams. Three hot gas filtration devices developed in the program by contractors were tested at METC to determine their performance in an actual hot gas stream produced by a small-scale, fluid-bed gasifier (2). The three devices were a Westinghouse ceramic cross-flow filter, an Acurex ceramic bag filter, and an electrostatic precipitator developed by Denver Research Institute. Details of the design of these devices and results of the work to date have been reported in a series of contractor review meetings (3-9).

Although the principal purpose of this series of tests was to measure the particulate removal efficiency of the hot gas filters at temperatures up to 1,850°F, they afforded the opportunity to also measure the concentration of 10 metals, which are common constituents of coal ash, in the gas stream. Specifically, it was desired to determine whether removal of particles from a coal gas at temperatures up to 1,850°F would affect the downstream concentration of trace species of metals such as sodium and potassium. The results of the experiment are reported in this paper.

Experimental

The low-Btu coal gas used during these tests was produced by METC's advanced concepts fluid-bed gasifier. The gasifier was designed to operate with a wide range of coals at pressures of 200 to 1,000 psig and temperatures up to 1,900°F. The gasifier is used as a source of low- to medium-Btu gas for use in testing downstream components and analytical instrumentation.

During these tests, the gasifier was operated at 400 psig with Montana Rosebud subbituminous coal, air, and steam to produce a gas of the following average composition:

N_2: 38.0 Percent
H_2O: 17.0 Percent
H_2: 17.0 Percent
CO: 13.5 Percent
CO_2: 10.0 Percent
CH_4: 3.5 Percent
H_2S: 0.3 Percent

Approximately 300 feet of insulated pipe separated the gasifier from the cleanup device test area. Heat loss and particle dropout in the pipe resulted in a gas temperature and solids loading that were lower than that required for the tests. Thus, a methane-fired heater was used to increase the temperature to the desired range (1,400° to 1,850°F), and a pressurized, screw-type particle feeder was used to feed particles into the gas stream up stream of the test device. These particles were obtained from a cyclone on the gasifier and had the same composition as the entrained particulate. The rate of particulate addition was varied depending on the amount already in the gas and the requirements of each test. Typically, the added particles were approximately 10 to 40 percent of the total at the inlet of the test devices. After exiting the cleanup device, the gas was cooled to remove condensibles, metered, and then incinerated.

Tests conducted with the Westinghouse and Acurex filters lasted 250 hours each. The test of the DRI electrostatic precipitator was terminated after approximately 50 hours because of a mechanical failure. During 50 hours of the Acurex filter test, the coal gas was desulfurized prior to particulate removal. This was accomplished using METC's hot gas desulfurization unit which uses a zinc ferrite ($ZnFe_2O_4$) sorbent to remove gaseous sulfur species. This device typically removes greater than 99 percent of the sulfur in the gas and produces gas streams with sulfur concentrations of less than 10 ppm (8). The configuration of the various components of the test system are shown in Figure 1.

Particulate sampling probes were positioned at various points in the system to characterize the performance of each device. To measure the solids loading of the gas produced by the gasifier, a sampling probe was placed in the gas line after the primary cyclone. Sampling probes were installed before and after the hot gas desulfurization unit to determine if this device removed particles from the gas stream or if zinc ferrite bed material was being lost by attrition.

The data reported here were collected at the inlet and outlet of the particulate removal test devices. The inlet probe was positioned downstream of the particle feeder, but upstream of the test device. The outlet sampling system was designed to filter the total system flow exiting the test device.

Sampling System Design

The inlet sampling probe was constructed of 1/4-inch stainless steel tubing with either a 0.035- or 0.049-inch wall thickness. The tip of the probe was beveled approximately 1/4 inch. When the probe was operated isokinetically, approximately 3 to 5 percent of the total process flow was sampled. The probe was positioned in a process pipe elbow with the probe tip approximately 6 inches upstream of the start of the bend.

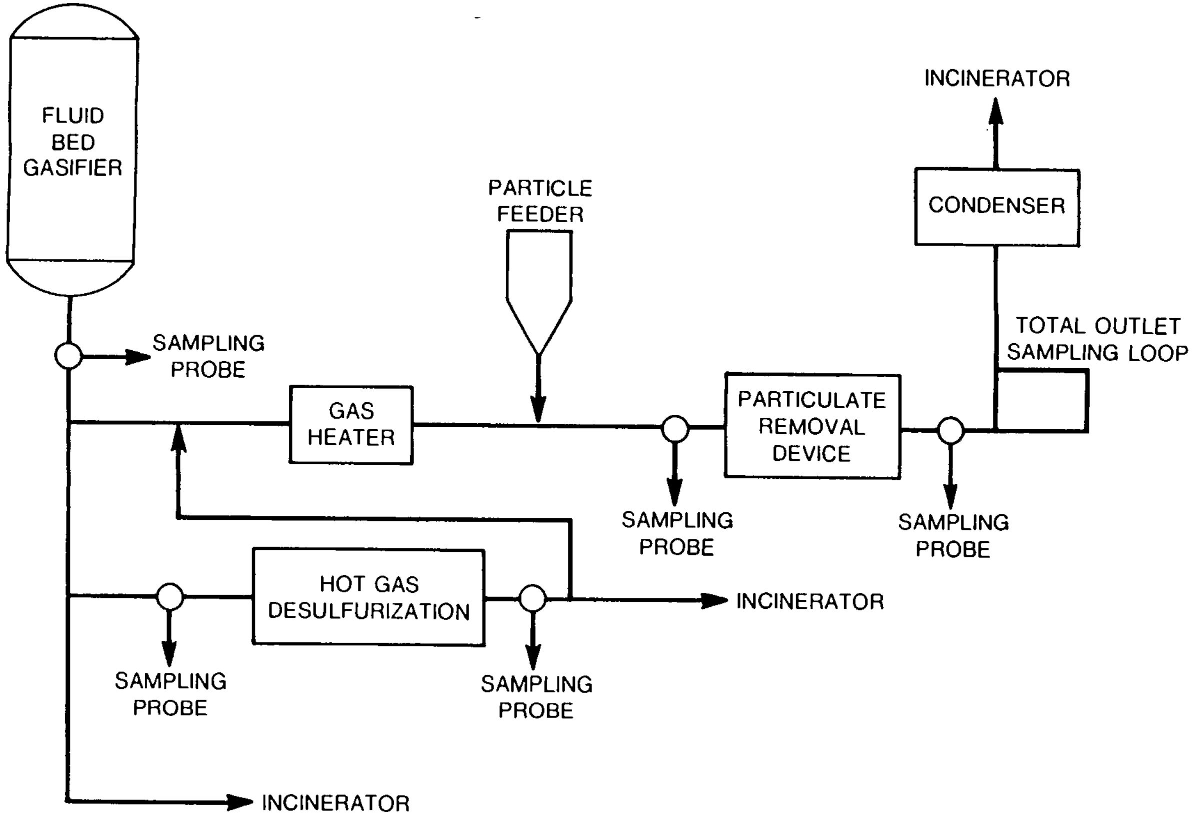
FLUID
BED
GASIFIER
SAMPLING
PROBE
GAS
HEATER
PARTICLE
FEEDER
SAMPLING
PROBE
PARTICULATE
REMOVAL
DEVICE
SAMPLING
PROBE
INCINERATOR
CONDENSER
TOTAL OUTLET
SAMPLING LOOP
HOT GAS
DESULFURIZATION
SAMPLING
PROBE
SAMPLING
PROBE
INCINERATOR
INCINERATOR

Figure 1
System Components

A-86-046-001 BP1-86

Figure 2 shows the inlet sample line configuration. The particulate samples were collected using 1.37- by 3.94-inch (35- by 100-millimeter), rounded bottom, alundum ceramic extraction thimbles (Norton No. 6406). The thimbles are designed to withstand temperatures up to 2,600°F, and pressure drops of up to 100 psi. The entire sampling line and gate valves were wrapped in high-temperature heating tapes, insulation, and a high-temperature glass cloth (Colombia Fiberglass). The heating tapes, controlled by digital temperature controllers (Omega Model No. CS4001KF), were maintained at 1,000°F. It was necessary to use an alternative heating method for the thimble holders because of their high mass. An 8-foot by 1/8-inch heating rod (ARI Industries, Inc.) was coiled around the elongated section of a thimble holder by means of metal hose clamps. The heating rods were powered from variable autotransformers set at 100 to 120 volts. The gas temperature at the downstream end of the thimble holders was typically 350° to 400°F for the inlet samples and 700° to 800°F for the outlet samples.

Approximately 30 feet of 3/8-inch stainless steel tubing separated the thimble holder from the flow monitoring system. This was necessary because of the shortage of available space in the test device area. The flow monitoring system consisted of a cooling coil, a condensate trap, and a flowmeter (rotameter). Condensate samples were collected in a 1-liter, stainless steel sampling cylinder (Hoke No. 8LD1000).

The flowmeter, a temperature indicator and a pressure gauge were located between two 1/4-inch needle valves. By adjusting these valves, the desired flow could be maintained at a known pressure and temperature. After metering, the gas was exhausted to an incinerator.

To take a particulate sample, the probe, gate valves, and thimble holder were first heated for 1 hour. Just prior to starting sample collection, the probe was purged with nitrogen for 3 to 5 seconds. The gate valves were opened and then the needle valves on the flow monitoring system were adjusted to set the sample gas flow rate. Sampling times were typically 1 to 2 hours.

After sample collection was completed, the thimble holders were disconnected and allowed to cool before removing the loaded thimble. The condensate was drained and measured so that the contribution of water vapor to the total gas flow could be calculated. The 30-foot section of tubing between the thimble holder and the flow monitoring system was purged with steam and nitrogen after each sample to remove residual condensate from the tubing walls. This was added to the condensate sample.

Figure 3 depicts the configuration of the total outlet sampling system. The sampling system was designed as a bypass loop from the main gas line. The entire gas flow was filtered using two thimble holders in parallel and then the gas was cooled to condense water vapor. The sample loop was isolated by gate valves (Vogt No. 821) upstream and downstream of the thimble holders. The sample loop and thimble holders were insulated and heated as described previously. The condensate was collected in stainless steel vessels which were drained before and just after each outlet sampling. The weight of the condensates was recorded so that the contribution of water vapor to the total gas flow could be calculated. Metal concentrations in the condensate could also be translated into equivalent total gas concentrations.

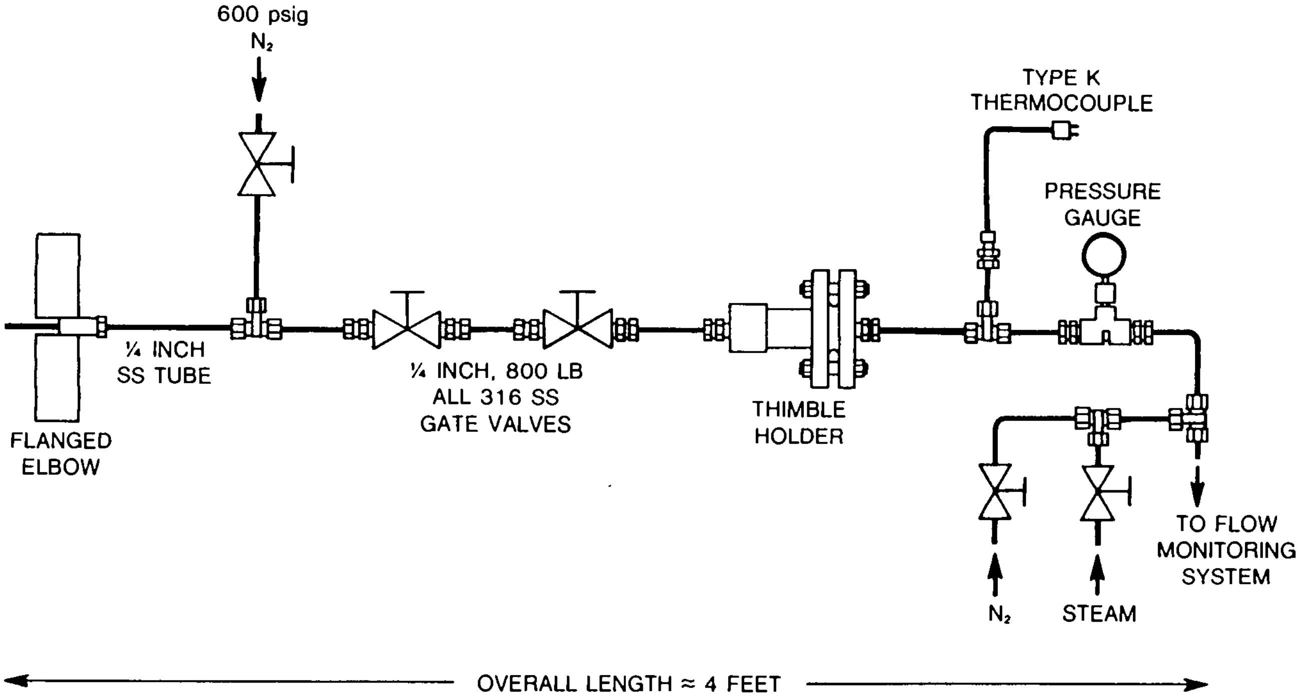
600 psig
N_2
TYPE K
THERMOCOUPLE
PRESSURE
GAUGE
¼ INCH
SS TUBE
FLANGED
ELBOW
¼ INCH, 800 LB
ALL 316 SS
GATE VALVES
THIMBLE
HOLDER
TO FLOW
MONITORING
SYSTEM
N_2
STEAM
OVERALL LENGTH ≈ 4 FEET

Figure 2
Sampling Probe Configuration

A-86-046-002 BP1-86

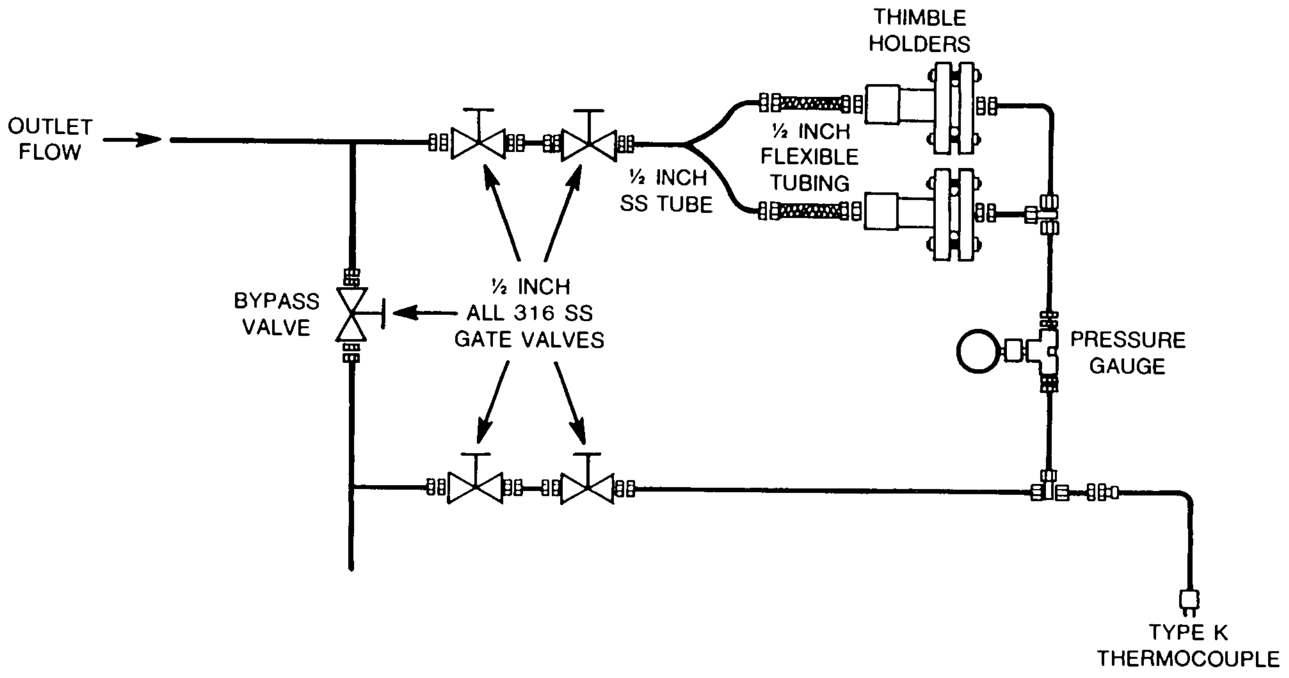
THIMBLE
HOLDERS
OUTLET
FLOW
½ INCH
FLEXIBLE
TUBING
½ INCH
SS TUBE
BYPASS
VALVE
½ INCH
ALL 316 SS
GATE VALVES
PRESSURE
GAUGE
TYPE K
THERMOCOUPLE

Figure 3
Total Outlet Sampling Configuration

A-86-046-004 BP1-86

Sample Preparation

Thimbles were heated in an oven at 250°F for approximately 30 minutes, cooled in a desiccator, and weighed on an analytical balance prior to being loaded into a thimble holder. After collecting a particulate sample, the thimble holders were extremely hot and were allowed to cool for approximately 30 minutes. The holder was then taken apart and the thimble removed. The thimble, containing the particulate sample, was placed in an oven at 250°F for approximately 45 minutes. After cooling, the thimble was weighed again. The difference in the initial and final weights was taken to be the weight of particles on the thimble. Typically, a small fraction of the particles escaped around the edge of a thimble while in the holder. These particles were collected together with the condensates and filtered out using Gelman Metricel, 47-millimeter, 0.45-micron, Type GA-6 filters under vacuum. The sample was then dried in an oven, cooled in a desiccator, and weighed. This weight was added to the weight of particles collected on the thimble to yield a total sample weight. Portions of the particles collected in the thimbles were submitted for particle size, ultimate, and metals analyses. Particles filtered from the condensates were not used for the chemical analyses because of the possibility that leaching had affected their composition. Particle size analyses were performed using a Model No. TAII Coulter Counter. The pH of the condensates was adjusted to $\leq$ 2.0 by addition of nitric acid, and stored in polyethylene bottles.

The solid and condensate samples were analyzed for 10 metals using a Perkin-Elmer Model 5000 atomic absorption spectrophotometer and a Spectrametrics, Inc., direct plasma atomic emission spectrometer. A lithium metaborate fusion was performed on the solid samples in order to generate a liquid for these analyses.

Data Analysis

As described in the experimental section, the concentrations of the metals in the gas stream were obtained by measuring their amounts in the particles and condensate collected utilizing sampling devices at the inlet and outlet of the test devices, and relating them to the quantity of gas which had flowed through the devices. In the course of the tests, 18 sets of inlet/outlet samples were taken for the Westinghouse ceramic cross-flow filter, 23 for the Acurex fabric bag filter, and 10 for the Denver Research Institute electrostatic precipitator.

The performance of the 3 filters are summarized in Table 1, which gives the average particulate loading of the inlet and outlet gas together with the calculated removal efficiency and the mean particle diameter. The average ultimate analyses of the particulate samples are detailed in Table 2, and Table 3 gives the average gas concentrations of particles, ash, and 10 metals. The calculated values of removal efficiency are also included.

Generally, the Westinghouse filter had the highest particulate removal efficiency followed by the Acurex and DRI filters. Removal efficiency tended to increase with inlet particle loading. The Westinghouse filter tended to result in a lower outlet particle loading than the Acurex or DRI filters because of its higher particulate removal efficiency.

Statistical analysis of the data indicates that, though not strong, there is a correlation between particulate removal efficiency and each of the metal removal efficiencies. The metal removal efficiencies significantly are some

2 to 6 percentage points lower, on average, than the particulate removal efficiency. This cannot be accounted for by gasification of carbon in the particulate on passing through the filters, for a similar result is obtained when compared with the ash removal efficiencies. This may be due to a higher metals concentration in the smaller particles passing through the filters.

A particularly interesting result is that metal removal efficiencies could not be shown to be dependent on operating conditions which varied in the ranges: temperature -- 800° to 1,600°F; pressure -- 140 to 250 psig; and flow rate -- 1,300 to 2,500 scfh. This is especially important for the case of the alkali metals, sodium and potassium, since it is speculated that, at higher temperatures and lower pressures, these relatively volatile species might pass more readily through the hot gas filters.

The average measured removal efficiency for the metals varied slightly among themselves. This is shown in Table 4. In Table 5, the metal concentrations are expressed as the average percentage of the total sum of the ten metals for both the inlet and outlet. These data show that there was an enrichment of Ca in the outlet gas. This was most apparent during the Westinghouse test during which the average Ca concentration increased from 20 percent of the total of the metals at the inlet to 28 percent of the total at the outlet. The source of this enrichment was believed to be the refractory lining of the piping. This assertion is supported by the fact that after the Westinghouse test, the original refractory was replaced with a new refractory that was rated for a higher temperature. Subsequently, during the Acurex and DRI tests Ca enrichment of the outlet gas continued but to a lesser degree. The outlet gas was enriched in Mg and alkalis as well, but to a lesser degree than Ca. These metals are also components of the refractory. The composition of the two refractories is shown in Table 6.

During 50 hours of the Acurex filter test, the hot gas to the filter was first desulfurized by passage through a fixed bed of zinc ferrite (8). The resulting gas tended to have a lower particulate loading comprising smaller size particles. No particulate was added to the gas stream during this period. However, the particulate removal efficiency during this period did not differ significantly from test periods when raw gas was utilized. Nor was it found that the particulate was enriched in zinc, which might have been a consequence of attrition or vaporization of the zinc ferrite bed. The only metal which showed a significant difference in removal efficiency during the test using desulfurized gas was nickel. The efficiency during the desulfurization test was lower.

TABLE 1. CHARACTERIZATION OF PARTICLES IN THE HOT COAL GAS STREAM

	Average Inlet Loading (mg/scf)	Average Outlet Loading (mg/scf)	Average Particulate Removal Efficiency %	Standard Deviation Removal Efficiency %	Average Inlet Mean Diameter (micron)	Average Outlet Mean Diameter (micron)
WESTINGHOUSE (18 samples)	65.91	0.86	98.15	1.42	9.76*	7.50**
ACUREX (23 samples)	64.38	1.91	95.59	4.38	8.76	7.00
DENVER RESEARCH INSTITUTE (10 samples)	72.36	5.03	93.29	4.25	8.84	8.70

* Inlet particulate size data available for 11 samples.

** Outlet particulate size data available for 10 samples.

TABLE 2. ULTIMATE ANALYSIS OF PARTICULATE SAMPLES

		Average Weight Percent				
Filter	Location	Ash	C	H	N	S
ACCUREX	Inlet	34.34	60.12	0.49	0.51	0.83
	Outlet	37.63	59.59	0.37	0.42	0.69
DRI	Inlet	39.34	55.10	0.38	0.69	1.20
	Outlet	38.18	56.94	0.30	0.69	0.85
WESTINGHOUSE	Inlet	34.61	58.22	0.53	0.88	1.36
	Outlet	39.94	55.47	0.44	0.87	1.36

TABLE 3. REMOVAL OF PARTICLES AND METALS FROM HOT COAL GAS

		Average Inlet Concentration (ppm)	Average Outlet Concentration (ppm)	Removal Efficiency (%)
WESTINGHOUSE	Particles	2,365.37	30.87	98.7
	Ash	742.00	12.40	98.3
	Al	105.27	1.75	98.3
	Ca	58.93	1.89	96.8
	Cr	2.62	0.07	97.3
	Cu	1.40	0.04	97.1
	Fe	91.09	2.29	97.5
	K	8.85	0.25	97.2
	Mg	21.08	0.46	97.8
	Na	4.62	0.12	97.4
	Ni	2.44	0.08	96.7
	Zn	0.84	0.03	96.4
ACUREX	Particles	2,310.50	68.55	97.0
	Ash	718.00	23.80	96.7
	Al	89.99	3.09	96.6
	Ca	48.51	2.40	95.1
	Cr	1.08	0.06	94.4
	Cu	1.53	0.04	97.4
	Fe	76.11	2.82	96.3
	K	8.89	0.47	94.7
	Mg	18.22	1.09	94.0
	Na	3.06	0.22	92.8
	Ni	0.61	0.05	91.8
	Zn	0.60	0.04	93.3
DRI	Particles	2,596.90	180.55	93.0
	Ash	969.00	57.7	94.0
	Al	173.61	23.59	86.4
	Ca	46.36	5.88	87.3
	Cr	0.92	0.10	89.1
	Cu	0.73	0.08	89.0
	Fe	113.89	12.80	88.8
	K	21.40	2.12	90.1
	Mg	15.50	2.49	83.9
	Na	5.75	0.72	87.5
	Ni	3.53	0.60	83.0
	Zn	0.62	0.06	90.3

TABLE 4

AVERAGE REMOVAL EFFICIENCIES FOR EACH METAL IN ORDER OF DECREASING EFFICIENCY

Metal	Number of Samples	Average Efficiency (%)
Al	50	93.89
Fe	51	93.73
Cr	51	93.21
K	51	92.83
Cu	51	92.37
Zn	51	91.89
Na	51	91.56
Ca	51	91.05
Mg	51	90.92
Ni	51	89.52

TABLE 5. AVERAGE INLET AND OUTLET PERCENT METAL COMPOSITIONS

		Average Metal Composition (% of Total of Ten Metals)			
Metal	Location	Acurex	DRI	Westinghouse	Average
Al	Inlet	35.50	46.16	32.30	36.46
	Outlet	27.73	42.72	25.22	29.78
Ca	Inlet	22.01	12.88	20.02	19.52
	Outlet	25.56	15.51	28.09	24.48
Cr	Inlet	0.64	0.26	1.45	0.85
	Outlet	0.87	0.47	1.15	0.89
Cu	Inlet	1.14	0.21	0.69	0.79
	Outlet	0.62	0.63	0.57	0.60
Fe	Inlet	27.18	28.15	31.78	28.99
	Outlet	25.43	23.10	30.14	26.64
K	Inlet	3.22	5.13	3.01	3.52
	Outlet	4.12	4.81	4.01	4.22
Mg	Inlet	8.19	4.34	7.39	7.15
	Outlet	10.24	8.49	7.07	8.78
Na	Inlet	1.28	1.49	1.69	1.47
	Outlet	4.20	1.92	1.91	2.94
Ni	Inlet	0.41	1.21	1.33	0.89
	Outlet	0.70	1.95	1.35	1.18
Zn	Inlet	0.44	0.18	0.35	0.36
	Outlet	0.52	0.41	0.50	0.49

TABLE 6. PIPELINE REFRACTORY COMPOSITIONS*

Test	Al_2O_3 %	SiO_2 %	Fe_2O_3 %	TiO_2 %	CaO %	MgO %	Alkalis %
Westinghouse[1]	13.95	30.29	5.34	0.14	35.39	8.81	2.92
Acurex, DRI[2]	38.61	31.48	5.38	1.50	19.54	0.79	1.41

* Plibrico Company Laboratory Report.

[1] Refractory maximum temperature rating was 1,500°F.

[2] Refractory maximum temperature rating was 2,000°F.

Conclusions

Analysis of inlet and outlet particulate samples in a hot coal gas stream passing through three different filtration devices indicates that 10 metals, commonly occurring in coal ash, were removed from the gas stream in proportion to the particulate removal. This remained true up to a temperature of 1,600°F, even for relatively volatile metals such as sodium and potassium. Metal removal efficiencies could not be shown to be dependent on operating conditions for temperatures up to 1,600°F, pressures up to 250 psig, and flow rates up to 2,500 scfh. The efficiency of removal of the metals was slightly less than the particulate removal efficiency, suggesting an enrichment of the metals in the smaller particles escaping through the filter.

References

1. Advanced Environmental Control Technology Program. Morgantown Energy Technology Center. 1981. Report No. DOE/METC/SP-187.

2. Evaluation of Three High-Temperature Particle Control Devices for Coal Gasification. Gas Cleaning at High Temperatures. The Institution of Chemical Engineers Symposium Series No. 99. R. J. Dellefield and R. C. Bedick. 1986.

3. High-Temperature, High-Pressure Particulate and Alkali Control in Coal Combustion Process Streams. K. E. Markel, Ed. 1981. Report No. DOE/MC/08333-167.

4. Second Annual Contractors' Meeting on Contaminant Control in Hot Coal-Derived Gas Streams. K. E. Markel, Ed. 1982. Report No. DOE/METC/82-47.

5. Third Annual Contractors' Meeting on Contaminant Control in Hot Coal-Derived Gas Streams. K. E. Markel, Ed. 1983. Report No. DOE/METC/84-6.

6. Fourth Annual Contractors' Meeting on Contaminant Control in Hot Coal-Derived Gas Streams. K. E. Markel, Ed. 1984. Report No. DOE/METC-85/3.

7. Fifth Annual Contractors' Meeting on Contaminant Control in Coal-Derived Gas Streams. D. C. Cicero and K. E. Markel, Eds. 1985. Report No. DOE/METC-85/6025.

8. Sixth Annual Contractors' Meeting on Contaminant Control in Hot Coal-Derived Gas Streams. K. E. Markel and D. C. Cicero, Eds. 1986. Report No. DOE/METC-86/6042.

9. Seventh Annual Contractors' Meeting on Gasification and Gas Stream Cleanup Systems. M. R. Ghate and K. E. Markel, Eds. 1987. Report No. DOE/METC-87/6079.

7B:4-28-87:dc:5b

OPPORTUNITIES FOR MEMBRANE SEPARATION PROCESSES IN COAL GASIFICATION

R.W. Baker, C.-M. Bell, I. Pinnau and J.G. Wijmans

Membrane Technology and Research, Inc.
1360 Willow Road, Menlo Park, CA 94025

The separation of hydrogen from synthesis gas is a major cost element in the manufacture of hydrogen from coal. Separation of these gases by membranes is an alternative technique that is still largely unexplored and that could offer substantial cost savings. We have been developing membranes for this application at Membrane Technology and Research, Inc. Most of this work has been supported by the U.S. Department of Energy.

There are three opportunities for membrane separation in the production of hydrogen from coal:

(1) The separation of hydrogen from carbon monoxide before the shift reactor.

(2) The separation of hydrogen from carbon dioxide and hydrogen sulfide after the shift reactor.

(3) The separation of hydrogen from nitrogen after the acid gas removal in an air-blown gasification process.

After reviewing polymer permeability data available in the literature or obtained at MTR, two polymers were selected for membrane development work:

(1) Poly(etherimide) for the separation of hydrogen from nitrogen and from carbon monoxide.

(2) Poly(ether-ester-amide) for the separation of hydrogen sulfide and carbon dioxide from hydrogen.

After characterizing the membrane properties of relatively thick (20-50 μm) films, we concentrated on fabricating asymmetric and composite ultrathin high-performance membranes. Asymmetric or composite ultrathin membranes in which the permselective layer is on the order of 0.5- to 1.0 μm-thick are required if usefully high membrane fluxes are to be obtained. The membranes were then tested with pure gases and gas mixtures.

POLY(ETHERIMIDE) MEMBRANES

The properties of the poly(etherimide) membranes are summarized in Figure 1. As shown, these membranes are extremely permeable to hydrogen compared to nitrogen and carbon monoxide. Poly(etherimide) membranes would, therefore, be most suitable for these separations. Poly(etherimide) is a tough, high-melting polymer. We have shown that the membranes maintain their desirable selectivity properties at temperatures in excess of 90°C. Membrane selectivity for gas mixtures is also essentially independent of feed gas composition, as the results in Figure 1 show. The membranes have been fabricated into continuous rolls of flat-sheet membranes and into hollow fibers.

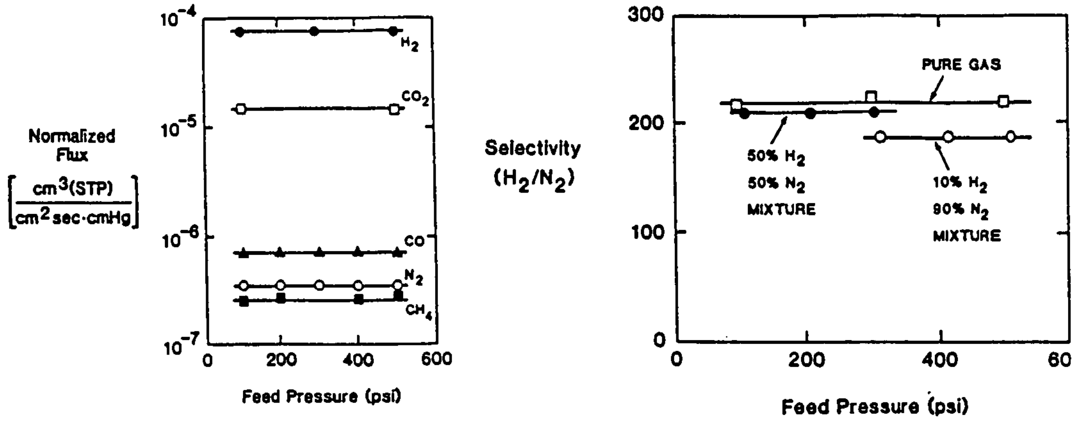

Figure 1. Normalized fluxes and selectivities of poly-(etherimide)/poly(dimethylsiloxane) composite membranes as a function of feed pressure. Temperature: 25°C.

POLY(ETHER-ESTER-AMIDE) MEMBRANES

Poly(ether-ester-amide) membranes are extremely selective for carbon dioxide, compared to other gases, as the data in Figure 2 show. Thus, these membranes are most suited to the separation of carbon dioxide from hydrogen/methane/nitrogen mixtures. Based on data from pure gases, a carbon dioxide/hydrogen selectivity greater than 10 would be expected. With gas mixtures, plasticization of the membrane by carbon dioxide lowers the selectivity to between 7 and 8. This mixed gas selectivity is lower than the pure gas selectivity, but still much higher than other polymeric membranes.

We have fabricated these poly(ether-ester-amide) membranes into spiral-wound membrane modules and tests with these modules are underway.

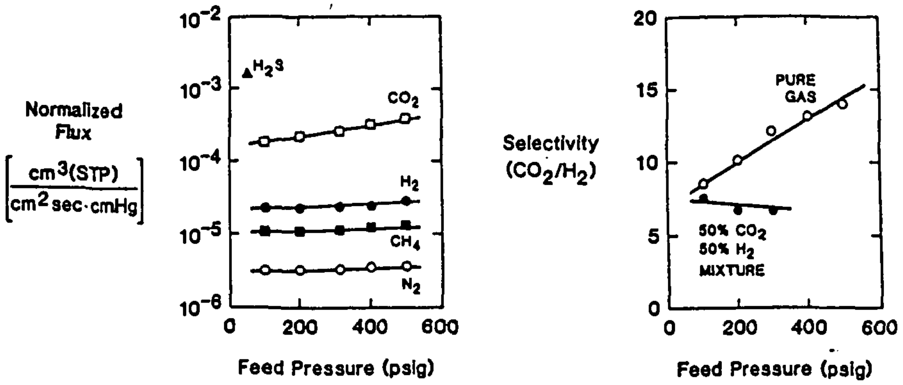

Figure 2. Normalized fluxes and selectivities of poly-(ether-ester-amide) composite membranes as a function of feed pressure. Temperature: 25°C.